PERTURBATION EFFECTS IN CAVITATION BUBBLE DYNAMICS

Thesis by

Maurice Rattray, Jr.

In Partial Fulfillment of the Requirements

For the Degree of

Doctor of Philosophy

California Institute of Technology

Pasadena, California

1951

ACKNOWLEDGMENTS

The writer wishes to thank Professor M. S. Plesset for suggesting this problem as a part of the extensive theoretical investigations being conducted at the Hydrodynamics Laboratory and for the many encouraging and helpful discussions which greatly aided the completion of this work.

This work was supported by the Office of Naval Research.

ABSTRACT

Previous theoretical investigations of cavitation bubble dynamics have failed to consider the effect of a nearby wall or of translatory motion of the bubble.

It is shown that these effects are not small, but actually the analysis based on this assumption finally breaks down due to the large deformation of the bubble in the later stages of collapse. However, as the major portion of the time of collapse is spent in the low velocity motion, a meaningful time of collapse is obtained which, for the case of a bubble against a wall, is 20% longer than in the symmetric case. This agrees with the experiments performed in the Hydrodynamics Laboratory at the California Institute of Technology. The time of collapse is not appreciably affected by a translatory motion of the bubble of the magnitude encountered in the above experiments.

TABLE OF CONTENTS

LIST OF TABLES

LIST OF FIGURES

I INTRODUCTION AND CONCLUSIONS

1:1. The Nature of Cavitation

Cavitation is the phenomenon present in liquids due to the occurrence of pockets of vapor phase called cavities or cavitation bubbles in a region of the liquid phase. Several examples of this are:

a. cavities produced by boiling,

b. cavities produced by flow over suitably shaped bodies,

c. cavities produced in the trailing vortices of propellers,

d. cavities produced by vibrating boundaries.

The essential criterion for cavitation is a region of liquid in which the pressure of the liquid is less than or equal to the vapor pressure. Thus, in boiling, the temperature is raised until the local vapor pressure reaches the liquid pressure, while in the other cases the fluid motion lowers the liquid pressure to vapor pressure in certain regions of flow.

For an empirical description of cavitation it is convenient to correlate experimental results with an appropriate dimensionless parameter called the cavitation parameter. Thoma,(1)* in his work on cavitation in pumps, defines a parameter

$$\sigma = \frac{P_s - P_v}{\Delta P}$$

where P_s = suction pressure of pump

P_v = vapor pressure of liquid corresponding to its temperature

* Numbers in parentheses refer to bibliography.

ΔP = pressure rise obtained from suction to discharge at the best efficiency point of pump.

This parameter has limited use as it varies from pump to pump and the definitions are not standardized. In cavitating flow about submerged bodies, the cavitation parameter is generally defined by

$$K = \frac{P_\infty - P_v}{\rho V_\infty^2/2}$$

where P_∞ = static pressure at a large distance from the body,

P_v = vapor pressure of liquid corresponding to its temperature,

ρ = liquid density,

V_∞ = uniform flow velocity at a large distance from the body.

Plesset(2) defines three regimes of flow over a body and qualitatively correlates them with the cavitation parameter. The first of these, noncavitating flow, occurs for sufficiently large values of K. This state of flow consists of the liquid phase only and obeys the well known laws of fluid mechanics. The second occurs for intermediate values of K and is described as cavitating flow with a relatively small number of cavitation bubbles in the field of flow. In this case a few bubbles form at the boundary of the body but the flow pattern is not appreciably altered from that found in noncavitating flow. The third regime, which occurs for sufficiently small K, is cavitating flow with a single large cavity about the body. The size of the cavity depends on K, with the larger cavities occurring for the smaller values of K, while the boundary of the cavity closely approximates a surface of constant pressure and constant flow speed. Photographs of the three regimes of flow, taken in the High Speed Water Tunnel in the Hydrodynamics Laboratory of the California Institute of Technology, are shown in Fig. 1.

In this study only the second regime of cavitation will be considered. This is of practical interest to designers of marine and hydraulic equipment for its presence increases the drag of a body in the fluid, decreases the efficiency of fluid propulsion systems, and can cause considerable damage to adjacent surfaces.

1:2. Experimental Investigations of Cavitation.*

Past experimental work on cavitation has been almost completely confined to problems related to the damage caused by the action of cavitation bubbles on various surfaces. The first study of this phenomenon was initiated in England by the Propeller Subcommittee of the Institute of Naval Architects in the year 1915. Their report(3) stated that the pitting on propellers was caused by the repeated hammering resulting from the collapse of small cavities formed adjacent to the moving blades. Since that time a considerable number of experimental investigations have been carried on, but as yet there has been no general agreement on the mechanism of the damaging action. Several different types of test apparatus have been used in these experiments. The Venturi tube and the Water Tunnel are used to give cavitation, but have the disadvantage that the production of damage is quite slow. In

---

* For a survey of the literature, see Schneider (4).

order to speed up this process a magnetostriction oscillator has been used in resonance with a column of water. In this manner very rapid production and collapse of bubbles is possible and the resulting damage greatly increased. From these investigations, estimates of the pressure ranging from 4,000[5,6,7] to 300,000[3,8,9] pounds per square inch have been reported. A sufficient number of experiments[8,9,10] have been performed, where chemical action must be negligible, to give strong support to the view that the destruction is almost entirely caused by mechanical action from the high pressures involved in cavitation bubble collapse.

Recently a series of remarkable photographs showing the life history of individual cavitation bubbles have been taken in the High Speed Water Tunnel in the Hydrodynamics Laboratory of the California Institute of Technology.[11] This equipment is well suited for cavitation research since it makes possible control of the production and collapse of the cavities to give reproducible results. The static pressure can be varied over the range 0.2 to 6.4 atmospheres, while the water velocity is adjustable from 0 to 90 ft. per sec. in steps of .09 ft. per sec. The working section is 89 1/2 in. long and has a diameter of 14 in. with sides of glass to allow observation of the models under operating conditions. A sketch of the water tunnel is shown in Fig. 2. Photographs of the bubbles have been taken on a moving film at a rate up to 20,000 per sec. A typical example is shown in Fig. 3.

1:3. Analytical Investigations of Cavitation.

Analytical studies of the collapse of bubbles were carried out by Cook[3] and Rayleigh,[12] independently, in 1917. These were based on an earlier work of Besant[13] who formulated the problem as follows:

> "An infinite mass of homogeneous incompressible fluid acted upon by no forces is at rest, and a spherical portion of the fluid is suddenly annihilated; it is required to find the instantaneous alteration of pressure at any point of the mass, and the time in which the cavity will be filled up, the pressure at an infinite distance being supposed to remain constant."

The main objection to these results* was the infinite velocities and pressures which were obtained at collapse. Various attempts have been made to eliminate the nonphysical infinite pressures and velocities, both by considering the liquid as compressible and by filling the cavity with gas or vapor which can only escape at a finite rate (4,14,15). As yet there has been no satisfactory general solution to this problem. However, these effects will not be appreciable for the greater portion of the bubble motion and good agreement between experiment and the calculations based on the incompressible case is to be expected.

Plesset[2] adapted the Rayleigh solution to the conditions obtained in the experiments of Knapp and Hollander. The pressure assumed in the calculation was taken to be the pressure measured at the appropriate point of the model surface just before the onset of cavitation. Figure 4 shows the measured pressure distribution and the comparison between the calculated and experimental motions. The general agreement is quite good, but the experimental time of collapse is consistently longer

---

* The results obtained by Rayleigh will appear as the zero order approximation in Part III.

than the calculated value. This discrepancy appears too soon in the motion to be due to any compressibility effects. The explanation of this disagreement will appear naturally from the results obtained in Part III.

1:4. Conclusions.

a. The causes of cavitation damage are primarily mechanical in nature.

b. The general features of cavitation bubble motion are understood.

c. There is need for a general method to take compressibility effects into account and thus avoid the infinities in the mathematical solution.

d. There is need for a more detailed understanding of the motion, which will explain the previous discrepancy between the theoretical and experimental times of collapse and also will explain the asymmetries observed in the laboratory. It is these questions which are considered in this work.

II OUTLINE OF THE PROBLEM

2:1 The Objective of this Investigation.

Since it is apparent that small perturbation effects may play an important role in the later stages of bubble collapse, and thus in cavitation damage, it was deemed worthwhile to investigate theoretically the results of several non-spherically symmetric conditions that are imposed in both the experiments performed in the Hydrodynamics Laboratory at the California Institute of Technology and in the natural occurrence of the phenomenon. It will be shown that the previously mentioned lifetime discrepancy is resolved by considering the effect of a nearby wall on the motion.

2:2. Conditions Assumed Throughout Motion.

For mathematical convenience, the motion of the bubble is calculated under the assumption that the interior of the bubble is a vacuum while the surrounding liquid is incompressible and inviscid. It is of interest to estimate the effect that these simplifying assymptions have on the motion in order to know what disagreement to expect between this theory and the experimental observations.

Compressibility of the liquid will have no appreciable effect on the motion until the velocities approach sonic speed. However, in the later stages of bubble collapse, the calculated values of pressure and velocity will be higher than those found experimentally, for some of the available energy will have been used in compression of the liquid. The asymmetries will accordingly be less than those calculated, but the time of collapse will not be appreciably changed as the greater portion of it is spent in the low velocity motion.

The interior of the bubble will actually consist of a mixture of vapor and the air. Since the initial air content of the bubble will of necessity be small, the maximum air content will depend on the rate of diffusion into the bubble during the growth process. This has been calculated by Epstein and Plesset [2] and shown to be negligible for this case. The effect of vapor is twofold: first, the condensation can only proceed at a finite rate; and secondly, the heat of condensation will raise the temperature in the neighborhood of the bubble. Plesset [2] finds that the effect of the finite condensation rate is negligible over the major portion of the collapse but will affect the motion in the later stages in the same manner as the compressibility does. He also considers the second effect and finds an insignificant temperature rise. Schneider [4] makes an estimate of the temperature rise in a slightly different way and arrives at the same conclusion.

To estimate the effect of surface tension, it is only necessary to compare the available energy due to surface tension with that from external pressure. The energy of a spherical cavity in a liquid is given by $4\pi R_o^2 \gamma$ for surface tension forces alone, and by $4/3\pi R_o^3 P_\infty$ for external pressure alone,

where R_o = the radius of the cavity,

γ = surface tension of the liquid,

P_∞ = pressure at the large distance from the cavity.

Thus the ratio of surface tension energy to energy from external pressure $= 3\gamma/R_o P_\infty$. For the experiments performed in the High Speed Water Tunnel, this has a value of approximately 4×10^{-3}, which is certainly negligible. Consequently no further consideration of surface tension effects will be included here.

2:3. Motion of a Bubble Over a Model Surface

When cavitation occurs, the cavities form in the regions of minimum pressure, which are always at a solid boundary in the experimental arrangements used with the High Speed Water Tunnel. The effects of this are several. First, there is a boundary layer at the solid wall; second, there is the possibility of adhesion to the wall; third, there is a pressure gradient in the vicinity of the wall; and fourth, the fluid does not extend to infinity in all directions.

Plesset[2], using the Blasius formula, estimates a boundary layer thickness of 6×10^{-3} inches for the experiments performed in the High Speed Water Tunnel. Since this is only 1/20 the maximum size of the bubble, the boundary layer will have little effect on the bubble motion. However, since the boundary layer is a region of constant pressure, the bubbles can be expected to form at random throughout this thickness instead of only at the boundary surface. The only noticeable effect of this would be to reduce the possibility of the bubble adhering to the wall.

No theoretical study of adhesion has been made, but experimentally it was shown by Van Iterson[16] that on a clean surface in water the angle of contact of a bubble is $22\ 1/2^{\circ}$ but when the surface is heavily greased with vaseline, this is increased to 90°. He then notices that the damage in a pump was greatly increased by operation in oily water. This he explained by saying that in the latter case the bubble adhered to the wall during its motion and thus collapsed right against it, while in the former, the bubble may have moved a little distance away from it. This effect would probably not be significant for the models used in the High Speed Water Tunnel, as here there is no reason for the bubble to migrate away from the wall, and, in fact, the presence of the wall has the reverse effect of attracting the collapsing bubble. However, in the laboratory there have appeared examples of distorted bubble shapes suggesting adhesion of the bubble to the surface.

Pressure gradients are present in the liquid both parallel and perpendicular to the model surface. Since the perpendicular change of pressure is small over the bubble dimensions, the asymmetries it produces will be small compared to those from other effects. The parallel gradient, on the other hand, will have a more marked effect as it will accelerate the liquid along the model surface. The net results of this will be translatory motion of the bubble through the fluid, which will correspond to an initial translatory motion of the fluid. Calculations for bubble collapse in this case are carried out in Part IV.

The presence of a wall near the bubble will restrict the fluid flow since no fluid can cross the wall surface. The effects of this on the collapse and growth of the bubble are calculated in Parts III and V, respectively.

III CALCULATION OF COLLAPSE IN THE VICINITY OF A WALL

3:1 The Coordinate System.

The coordinate system is set up with an origin placed in the bubble and with the outward pointing normal to the wall as the positive z-axis. Polar coordinates r, θ, ϕ, are defined in the usual manner, but since the problem is symmetric about the z-axis the ϕ coordinate is eliminated from further consideration. The radius of the bubble is assumed to be given by

$$R = \sum_{n=0}^{\infty} R_n(t) P_n(\cos\theta) \qquad (1)$$

where the $R_n(t)$ are functions only of time, to be determined by the problem. We define the position of the origin in such a manner that $R_1 \equiv 0$ throughout the motion. Then the distance from the origin to the wall is given by $D\left[1 - X(t)\right]/2$ where D is constant such that D/2 is the initial distance to the wall. The motion of the centroid of the bubble is given by the change in the variable X(t) which depends on the time only. This coordinate system is illustrated in Fig. 5.

3:2. The Differential Equations.

The solution of the problem consists in the simultaneous solution of two simpler problems: the calculation of the fluid motion, supposing that the boundary motion is known; and the calculation of the boundary motion, supposing the fluid motion known.

Since the fluid is assumed incompressible, inviscid, and initially at rest, the motion will be irrotational. Under these conditions, the equation of continuity takes[17] the form:

$$\nabla^2 \Phi(r,\theta,t) = 0, \qquad (1)$$

where Φ is the velocity potential of the motion, such that the velocity of the fluid with respect to a fixed reference system is given by:

$$\overline{V}(r,\theta,t) = -\nabla\Phi(r,\theta,t) \tag{2}$$

The ∇ in these equations is taken with respect to the moving coordinate system with the origin in the bubble as specified in 3:1. Now the r and θ components of the velocity $\overline{q}$ of the fluid relative to the moving coordinate system can be written as:

$$\begin{aligned} q_r(r,\theta,t) &= v_r(r,\theta,t)-v_o(t)\cos\theta, \\ q_\theta(r,\theta,t) &= v_\theta(r,\theta,t)+v_o(t)\sin\theta, \end{aligned} \tag{3}$$

where $v_o(t)$ is the velocity of the moving origin and is directed along the z-axis.

The equation for the motion of the boundary will be determined from the fact that the bubble surface must always contain the same particles of fluid. If the boundary is given as $f(r,\theta,t) = 0$, the condition that it always contains the same particles is given[17] by:

$$\frac{df}{dt} = \frac{\partial f}{\partial t} + \overline{q}\cdot\nabla f = 0 \tag{4}$$

The form of f is assumed in 3:1 to be

$$r - R(\theta,t) = 0. \tag{5}$$

Thus equation (4) becomes:

$$\dot{R} = q_r - q_\theta \frac{1}{R}\frac{R}{\theta}, \tag{6}$$

where the dot is used to represent partial differentiation with respect to time.

The differential equations (1) and (6) are to be solved with the appropriate boundary and initial conditions.

3:3. The Boundary Conditions

The boundary conditions on the fluid are: the velocity must be zero at an infinite distance from the cavity, the z component of velocity must be zero on the wall, and the pressure must be zero on the bubble surface and constant at large distances from the bubble. These are expressed analytically as follows:

$$\bar{v} = -\nabla\Phi = 0, \text{ at } r = \infty \tag{1}$$

$$v_z = -\frac{\partial \Phi}{\partial z} = 0, \text{ at } z = -D(1-X)/2, \tag{2}$$

$$p = 0 \quad , \text{ at } r = R, \tag{3}$$

$$p = P_\infty > 0 \quad , \text{ at } r = \infty, \tag{3'}$$

where $p(r,\theta,t)$ is the pressure of the liquid. The first two conditions are expressed in terms of Φ , but the problem remains to express (3) in a corresponding manner. In order to do this, one uses the momentum relation[17]:

$$\frac{d}{dt}\rho\bar{v} = -\nabla p, \tag{4}$$

where ρ is the constant fluid density. Writing out the left side and dividing by ρ gives:

$$\frac{\partial}{\partial t}\bar{v} + (\bar{q}\cdot\nabla)\bar{v} = -\frac{1}{\rho}\nabla p$$

Substituting $\bar{v} = -\nabla\Phi$ in the first term and $\bar{v} = \bar{q} + \bar{e}_z v_o$ in the second, where $\bar{e}_z$ is the unit vector in the z direction, one gets

$$-\frac{\partial}{\partial t}\nabla\Phi+(\bar{q}\cdot\nabla)(\bar{q}+\bar{e}_z v_o)=-\frac{1}{\rho}\nabla p.$$

An interchange of the order of differentiation in the first term and the use of the fact that $\nabla\, \bar{e}_z v_o = 0$ gives:

$$-\nabla\frac{\partial\Phi}{\partial t}+(\bar{q}\cdot\nabla)\bar{q}=-\frac{1}{\rho}\nabla p$$

or

$$\nabla\left[-\frac{\partial\Phi}{\partial t}+\frac{1}{2}q^2\right]=\nabla\left[-p/\rho\right].$$

Integration gives

$$-\frac{\partial\Phi}{\partial t}+\frac{1}{2}q^2=-p/\rho+C(t), \tag{5}$$

where C(t) is an integration constant which depends on t. To evaluate C(t), the equation is applied to the fluid at infinity. Since the velocity at infinity is zero, it follows that $q^2 = v_o^2$ and Φ is independent of the space coordinates and can be set equal to zero. If the pressure at infinity is denoted by P_∞, then equation (5) becomes:

$$\frac{1}{2}v_o^2=-\frac{P_\infty}{\rho}+C(t)$$

or

$$C(t)=\frac{1}{2}v_o^2+\frac{P_\infty}{\rho}.$$

Substituting this value back into equation (5) gives:

$$-\frac{\partial\Phi}{\partial t}+\frac{1}{2}q^2=\frac{P_\infty-p}{\rho}+\frac{1}{2}v_o^2. \tag{6}$$

Thus equation (3) gives the following condition on Φ at r = R:

$$-\frac{\partial \Phi}{\partial t} + \frac{1}{2}q^2 = \frac{P_\infty}{\rho} + \frac{1}{2}V_0^2. \tag{7}$$

The units can be chosen so that $P_\infty/\rho = 1$ with no loss in generality. Then

$$-\frac{\partial \Phi}{\partial t} + \frac{1}{2}q^2 = 1 + \frac{1}{2}V_0^2 \tag{8}$$

at r = R.

3:4. The Initial Conditions

The initial conditions are that the fluid velocity is zero and that the cavity is a sphere of radius unity with its center a distance D/2 from the wall. Choosing the initial radius as unity involves no loss in generality as it is arbitrary what length is to be called the unit distance.

3:5. The Calculations

A general solution of equation 3:2(1), valid for the region outside the bubble and satisfying condition 3:3(1), is given by

$$\Phi = \sum_{n=0}^{\infty} \frac{\phi_n(t)}{r^{n+1}} P_n(\cos\theta), \tag{1}$$

where the $P_n(\cos\theta)$ are the Legendre polynomials, and the $\Phi_n(t)$ are functions of time only, to be determined by the problem. The most convenient way in which to satisfy condition 3:3(2) is to form the image potential of equation (1).

It will be shown by induction that the image potential of

$$\frac{P_n \cos\theta}{r^{n+1}}$$

making the wall a streamline is

$$\sum_{m=0}^{\infty}(-1)^{n+m}\frac{(n+m)!}{n!m!}\frac{r^m}{D^{m+n}}P_m(\cos\theta), \tag{2}$$

which is a valid solution of equation 3:3(1) for $r < D$, where $D/2$ is the distance from the origin to the wall. Suppose first that this relation is true for all $n \leqslant N$. Then it must be shown that it also holds for $n = N + 1$. Consider the potential

$$\frac{\partial}{\partial z}\frac{P_N(\cos\theta)}{r^{N+1}} \tag{3}$$

The image potential must be, from equation (2), with $n = N$,

$$-\frac{\partial}{\partial z}\sum_{m=0}^{\infty}(-1)^{N+m}\frac{(N+m)!}{N!m!}\frac{r^m}{D^{N+m}}P_m(\cos\theta), \tag{4}$$

since this operation retains the symmetry about the wall required for the image potential.

Now

$$\frac{\partial}{\partial z} = \frac{\partial r}{\partial z}\frac{\partial}{\partial r} + \frac{\partial \theta}{\partial z}\frac{\partial}{\partial \theta}$$

$$= \cos\theta \frac{\partial}{\partial r} - \frac{\sin\theta}{r}\frac{\partial}{\partial \theta} \;.$$

Thus equation (3) gives:

$$\frac{\partial}{\partial z} \; \frac{P_N(\cos\theta)}{r^{N+1}} =$$

$$\frac{1}{r^{N+2}}\left[-(N+1)\cos\theta\, P_N(\cos\theta) + \sin^2\theta\, P_N'(\cos\theta)\right].$$

Now, by the relations between Legendre functions,[18] this can be simplified to:

$$\frac{\partial}{\partial z} \; \frac{P_N(\cos\theta)}{r^{N+1}} = -(N+1)\,\frac{P_{N+1}(\cos\theta)}{r^{N+2}} \,. \tag{5}$$

Application of the same method to equation (4) gives:

$$-\frac{\partial}{\partial z}\sum_{m=0}^{\infty}(-1)^{N+m}\frac{(N+m)!}{N!m!}\frac{r^m}{D^{N+m}}\,P_m(\cos\theta) =$$

$$\sum_{m=1}^{\infty}(-1)^{N+m+1}\frac{(N+m)!}{N!m!}\frac{r^{m-1}}{D^{N+m}}\left[m\cos\theta\, P_m(\cos\theta) + \sin^2\theta\, P_m'(\cos\theta)\right],$$

the m = 0 term dropping out as it is a constant. By substituting m' = m - 1 and then dropping the prime, one obtains:

$$\sum_{m=0}^{\infty}(-1)^{N+m+2}\frac{(N+m+1)!}{N!(m+1)!}\frac{r^m}{D^{N+m+1}}\left[(m+1)\cos\theta\, P_{m+1}(\cos\theta)+\sin^2\theta\, P'_{m+1}(\cos\theta)\right]$$

This simplifies to:

$$-\frac{\partial}{\partial z}\sum_{m=0}^{\infty}(-1)^{N+m}\frac{(N+m)!}{N!m!}\frac{r^m}{D^{N+m}}P_m(\cos\theta) = \tag{6}$$

$$\sum_{m=0}^{\infty}(-1)^{N+m+2}\frac{(N+m+1)!}{N!\,m!}\frac{r^m}{D^{N+m+1}}P_m(\cos\theta).$$

Comparison of equations (5) and (6) shows that the image of

$$\frac{P_{N+1}(\cos\theta)}{r^{N+2}}$$

is

$$\sum_{m=0}^{\infty}(-1)^{N+m+1}\frac{(N+m+1)!}{(N+1)!\,m!}\frac{r^m}{D^{N+m+1}}P_m(\cos\theta),$$

which is the same as equation (2). Now the image of the potential $1/r$, which makes the wall a streamline(18) is:

$$\sum_{m=0}^{\infty}(-1)^m\frac{r^m}{D^m}P_m(\cos\theta).$$

Since this is the $n = 0$ case of equation (2), the proposition is proved.

In the problem at hand the distance to the wall is $D(1 - X)/2$. Thus a solution of equation 3:2(1) valid outside the bubble for $r < D(1-X)$ which also satisfies condition 3:3(2) is:

$$\Phi = \sum_{n=0}^{\infty} \frac{\Phi_n}{r^{n+1}} P_n(\cos\theta) + \sum_{n=0}^{\infty} \sum_{m=0}^{\infty} (-1)^{n+m} \frac{(n+m)!}{n!m!} \frac{\Phi_n}{D^n(1-X)^n} \left[\frac{r}{D(1-X)}\right]^m P_m(\cos\theta). \tag{7}$$

The procedure for solution is then to substitute expressions 3:1(1) and 3:5(7) for R and Φ into equations 3:2(6) and 3:3(8) which hold at $r = R$. In this manner two first order differential equations are obtained, each containing terms in $P_n(\cos\theta)$. Since these equations must be valid over the entire range of θ and since the $P_n(\cos\theta)$ are an orthogonal set, it is necessary that the terms in each $P_n(\cos\theta)$ independently satisfy the equations.

The solutions to the problem must depend on the initial distance from the bubble to the wall. To express this analytically it is convenient to define a parameter $h = 1/D$ which always is less than or equal to 1/2, from the definition of D. It is now assumed that R_n and Φ_n are functions of h, that can be expanded into a Taylor's series about the spherically symmetric case of $h = 0$, as follows:

$$R_n = \sum_{m=0}^{\infty} h^m R_n^{(m)}(R_o),$$

$$\Phi_n = \sum_{m=0}^{\infty} h^m \Phi_n^{(m)}(R_o), \qquad (8)$$

$$X_n = \sum_{m=0}^{\infty} h^m X^{(m)}(R_o),$$

where h depends only on the initial conditions of the problem and $R_n^{(m)}(R_o)$, $\Phi_n^{(m)}(R_o)$, $X^{(m)}(R_o)$ are functions of R_o only. Then the coefficients of equal powers of h are equated to give the differential equations for $R_n^{(m)}$, $\Phi_n^{(m)}$, $X_n^{(m)}$. These are simultaneous first order equations which can be solved in pairs from the given initial conditions.

The calculations will be done step by step starting with the h-independent terms, then considering all terms up to and including ever increasing powers of h. The calculations have been carried out up to h^6, but it is deemed sufficient here to show the calculations only up to h^4, since the expressions rapidly become exceedingly unwieldy with increasing order of h.

It will be assumed from physical arguments that $|X| < 1$ and $\left|\frac{R-R_o}{R_o}\right| < 1$. In the following work, binomial expansions in terms of these quantities will be used freely with the justification to appear from their calculated values.

Considering only terms independent of h, one has equations of the following form. Equation (7) takes the form

$$\Phi = \frac{\Phi_o}{r} + O(h),$$

and equation 3:1(1) the form

$$R = R_o + O(h).$$

Equation 3:3(8) becomes

$$-\frac{\dot{\Phi}_o}{R_o} + \frac{1}{2}q^2 = 1 + O(h), \tag{9}$$

while from 3:2(6) and 3:2(3)

$$\begin{aligned} \dot{R}_o &= q_r + O(h) = q + O(h) \\ &= V_r + O(h) = -\frac{\partial \Phi}{\partial r} + O(h) \\ &= \frac{\Phi_o}{R_o^2} + O(h), \end{aligned} \tag{10}$$

with q, q_r, and v_r all evaluated at r = R. At this point it is convenient to change the independent variable from t to R_o. Since in this problem R_o is a monotone decreasing function of t, the change of variable is single valued and can be given by the expression

$$t = \sum_{m=0}^{\infty} h^m t^{(m)}(R_o). \tag{8'}$$

Now, with use of equation (10), equation (9) becomes

$$-\frac{\dot{\Phi}_o}{R_o^3}\frac{d\Phi_o^{(0)}}{dR_o} + \frac{1}{2}\frac{\Phi_o^2}{R_o^4} = 1 + O(h).$$

Expanding as in equation (8) and equating the h-independent terms, one obtains

$$-\frac{\Phi_o^{(0)}}{R_o^3}\frac{d\Phi_o^{(0)}}{dR_o}+\frac{1}{2}\frac{\{\Phi_o^{(0)}\}^2}{R_o^4}=1\,. \tag{11}$$

Multiplying through by R_o^2, one finds

$$-\frac{\Phi_o^{(0)}}{R_o}\frac{d\Phi_o^{(0)}}{dR_o}+\frac{1}{2}\frac{\{\Phi_o^{(0)}\}}{R_o^2}=R_o^2\,,$$

or,

$$-\frac{1}{2}\frac{d}{dR_o}\left[\frac{\{\Phi_o^{(0)}\}^2}{R_o}\right]=\frac{1}{3}R_o^3\,.$$

Integration gives

$$-\frac{1}{2}\frac{\{\Phi_o^{(0)}\}^2}{R_o}=\frac{1}{3}(R_o^3-1)\,,$$

where the constant of integration is determined by the initial conditions. Thus

$$\Phi_o^{(0)}=-\sqrt{\tfrac{2}{3}R_o(1-R_o^3)}\,, \tag{12}$$

where the sign is chosen for the case of a collapsing bubble.

The time of collapse is given by

$$\mathcal{T}=\sum_{m=0}^{\infty}h^m\,\mathcal{T}^{(m)}\,, \tag{8''}$$

where

$$\mathcal{T}^{(m)}=\int_1^0\frac{dt^{(m)}}{dR_o}\,dR_o\,.$$

$\tau^{(0)}$ can be found by combining equations (8), (10), and (11) to give

$$\frac{dt^{(0)}}{dR_0} = \frac{R_0^2}{\Phi_0^{(0)}} = -\frac{R_0^2}{\sqrt{\frac{2}{3}R_0(1-R_0^3)}}$$

Therefore

$$\tau^{(0)} = \int_1^0 \frac{-R_0^2\,dR_0}{\sqrt{\frac{2}{3}R_0(1-R_0^3)}}$$

$$= .915$$

This is the Rayleigh solution.

Considering only terms independent of h^2 and higher powers, one proceeds in a similar manner. Equation (7) becomes

$$\Phi = \frac{\Phi_0}{r} + \frac{\Phi_0}{D(1-X)} + O(h^2)$$

and equation 3:1(1) becomes

$$R = R_0 + O(h^2)$$

since no terms in $\Phi_0 P_1$ (cose0) appear to this order, and therefore it is not necessary to introduce Φ_1 to satisfy the ensuing equations. Thus Φ_1 is $O(h^2)$ which gives $v_0 = O(h^2)$ and $X = O(h^3)$ since $v_0 = -D\dot{X}/2$.

Now equation 3:3(8) becomes

$$-\frac{\dot{\Phi}_0}{R_0}-\frac{\dot{\Phi}_0}{D}+\frac{1}{2}q^2=1+O(h^2), \tag{13}$$

and equation 3:2(6) becomes with equation 3:2(3)

$$\dot{R}_0=q_r+O(h^2)=q+O(h^2)$$

$$=V_r+O(h^2)=V+O(h^2).$$

From equation 3:2(2)

$$\dot{R}_0=\frac{\Phi_0}{R_0^2}+O(h^2)=q+O(h^2) \tag{14}$$

Substitution of equation (14) into equation (13) gives

$$\left(-\frac{1}{R_0}-\frac{1}{D}\right)\dot{\Phi}_0+\frac{1}{2}\left\{\frac{\Phi_0}{R_0^2}\right\}^2=1+O(h^2).$$

When the independent variable is changed from t to R_0, one gets

$$-\frac{\Phi_0}{R_0^2}\left(\frac{1}{R_0}+\frac{1}{D}\right)\frac{d\Phi_0}{dR_0}+\frac{1}{2}\left\{\frac{\Phi_0}{R_0^2}\right\}^2=1+O(h^2).$$

With the use of equation (8), this equation becomes

$$-\frac{\Phi_0^{(0)}+h\Phi_0^{(1)}}{R_0^2}\left(\frac{1}{R_0}+h\right)\frac{d}{dR_0}\left[\Phi_0^{(0)}+h\Phi_0^{(1)}\right]$$

$$+\frac{1}{2}\left\{\frac{\Phi_0^{(0)}+h\Phi_0^{(1)}}{R_0^2}\right\}^2=1+O(h^2).$$

Equating the coefficients of h^0 gives equation (11). Equating the coefficients of h^1 gives

$$-\frac{\Phi_0^{(0)}}{R_0^3}\frac{d\Phi_0^{(1)}}{dR_0}-\frac{\Phi_0^{(0)}}{R_0^2}\frac{d\Phi_0^{(0)}}{dR_0}-\frac{\Phi_0^{(1)}}{R_0^3}\frac{d\Phi_0^{(0)}}{dR_0}+\frac{\Phi_0^{(0)}\Phi_0^{(1)}}{R_0^4}=0 \tag{15}$$

which has the solution

$$\Phi_0^{(1)}=-\tfrac{1}{2}R_0\Phi_0^{(0)} \tag{16}$$

Inverting equation (14) gives

$$\frac{dt}{dR_0}=\frac{R_0^2}{\Phi_0}+O(h^2).$$

Expanding in powers of h and considering coefficients of h^1, one obtains with the aid of equation (16)

$$\frac{dt^{(1)}}{dR_0}=\frac{R_0^2\cdot\frac{1}{2}R_0}{\Phi_0^{(0)}}$$

Thus

$$\tau^{(1)}=\int_1^0\frac{1}{2}\frac{R_0^3}{\Phi_0^{(0)}}dR_0$$

$$=0.41\,\tau^{(0)}$$

The time of collapse is therefore

$$\tau=.915(1+0.41h)+O(h^2). \tag{17}$$

For each higher power of h included, another term in the Legendre polynomial expansions for Φ and R will appear. Thus

$$\Phi_1 = O(h^2), \qquad v_o = O(h^2),$$

$$\Phi_2 = O(h^3), \qquad R_2 = O(h^3),$$

$$\Phi_3 = O(h^4), \qquad R_3 = O(h^4), \quad \text{etc.}$$

With this knowledge it is possible to solve the equations up to $O(h^4)$ in one step. This is done in the following.

Considering all terms up to and including those of $O(h^4)$, one can write equation (7)

$$\begin{aligned}\Phi = {} & \frac{\Phi_0}{r} + \frac{\Phi_1}{r^2} P_1(\cos\theta) + \frac{\Phi_2}{r^3} P_2(\cos\theta) \\ & + \frac{\Phi_3}{r^4} P_3(\cos\theta) + \frac{\Phi_0}{D(1-x)} - \frac{\Phi_0 r}{D^2(1-x)^2} P_1(\cos\theta) \\ & + \frac{\Phi_0 r^2}{D^3(1-x)^3} P_2(\cos\theta) - \frac{\Phi_0 r^3}{D^4(1-x)^4} P_3(\cos\theta) \\ & - \frac{\Phi_1}{D^2(1-x)^2} + O(h^5),\end{aligned} \tag{18}$$

and equation 3:1(1)

$$R = R_0 + R_2 P_2(\cos\theta) + R_3 P_3(\cos\theta) + O(h^5) \tag{19}$$

Substitution of equation 3:2 (3) in 3:2(6) gives, when the terms are evaluated at r = R,

$$\dot{R} = V_r - V_0 \cos\theta - \frac{1}{R}\left(V_\theta + V_0 \sin\theta\right)\frac{\partial R}{\partial \theta} \tag{20}$$

From this equation and the condition that $R_1 = 0$, the expression for v_o will be found. The first step is to evaluate each of the terms in equation (20) to terms of $O(h^4)$. Since v_o and v_o are $O(h^2)$ and $\partial R/\partial\theta$ is $O(h^3)$, the right hand term of equation (20) can be neglected to $O(h^4)$. Thus from equations (19) and (20)

$$\begin{aligned}\dot{R} &= \dot{R}_0 + \dot{R}_2 P_2(\cos\theta) + \dot{R}_3 P_3(\cos\theta) + O(h^5) \\ &= V_r - V_0 \cos\theta + O(h^5) \\ &= -\frac{\partial \Phi}{\partial r} - V_0 \cos\theta + O(h^5),\end{aligned} \tag{21}$$

evaluated at r = R.

Substituting for Φ from equation (18), one gets

$$\begin{aligned}\dot{R} = {} & \frac{\Phi_0}{R^2} + \frac{2\Phi_1}{R^3} P_1(\cos\theta) + \frac{3\Phi_2}{R^4} P_2(\cos\theta) \\ & + \frac{4\Phi_3}{R^5} P_3(\cos\theta) + \frac{\Phi_0}{D^2(1-X)^2} P_1(\cos\theta) \\ & - \frac{2\Phi_0 R}{D^3(1-X)^3} P_2(\cos\theta) + \frac{3\Phi_0 R_2}{D^4(1-X)^4} P_3(\cos\theta) \\ & - V_0 \cos\theta + O(h^5).\end{aligned}$$

Substituting for R from equation (19) and simplifying, one finds

$$\dot{R} = \frac{\Phi_0}{R_0^2} + P_1(\cos\theta)\left\{\frac{2\Phi_1}{R_0^3} + \frac{\Phi_0}{D^2} - V_0\right\}$$
$$+ P_2(\cos\theta)\left\{-\frac{2\Phi_0 R_2}{R_0^3} + \frac{3\Phi_2}{R_0^4} - \frac{2\Phi_0 R_0}{D^3}\right\}$$
$$+ P_3(\cos\theta)\left\{-\frac{2\Phi_0 R_3}{R_0^3} + \frac{4\Phi_3}{R_0^5} + \frac{3\Phi_0 R_0^2}{D^4}\right\} \qquad (22)$$
$$+ O(h^5).$$

Upon comparison of equations (21) and (22), the following identities are established:

$$V_0 = \frac{2\Phi_1}{R_0^3} + \frac{\Phi_0}{D^2} + O(h^5), \qquad (23)$$

$$\dot{R}_0 = \frac{\Phi_0}{R_0^2} + O(h^5), \qquad (24)$$

$$\dot{R}_2 = \frac{-2\Phi_0 R_2}{R_0^3} + \frac{3\Phi_2}{R_0^4} - \frac{2\Phi_0 R_0}{D^3} + O(h^5), \qquad (25)$$

$$\dot{R}_3 = \frac{-2\Phi_0 R_3}{R_0^3} + \frac{4\Phi_3}{R_0^5} + \frac{3\Phi_0 R_0^2}{D^4} + O(h^5), \qquad (26)$$

From equation 3:2(2) evaluated at r = R,

$$V_\theta = \frac{\sin\theta}{R}\left\{\frac{\Phi_1}{R^2} - \frac{\Phi_0 R}{D^2}\right\} + O(h^3).$$

Substituting for R from equation (19) and simplifying, one obtains

$$V_\theta = \left\{\frac{\Phi_1}{R_0^3} - \frac{\Phi_0}{D^2}\right\}\sin\theta + O(h^3).$$

Thus, from equations 3:2(3) and (23),

$$q_\theta = V_\theta + V_0 \sin\theta = \frac{3\Phi_1}{R_0^3}\sin\theta + O(h^3). \tag{27}$$

Equation 3:3(8) gives

$$-\frac{\partial \Phi}{\partial t} + \frac{1}{2}q^2 = 1 + \frac{1}{2}V_0^2$$

at r = R. This equation is to be broken down into its component parts by taking each term, expressing it as a sum of Legendre polynomials and then combining terms according to this equation. From equation (18),

$$\begin{aligned}
-\frac{\partial \Phi}{\partial t} = &-\frac{\dot{\Phi}_0}{R} - \frac{\dot{\Phi}_1}{R^2}P_1(\cos\theta) - \frac{\dot{\Phi}_2}{R^3}P_2(\cos\theta) \\
&- \frac{\dot{\Phi}_3}{R^4}P_3(\cos\theta) - \frac{\dot{\Phi}_0}{D(1-x)} - \frac{\Phi_0\dot{x}}{D(1-x)^2} \\
&+ \frac{\dot{\Phi}_0 R}{D^2(1-x)^2}P_1(\cos\theta) + \frac{2\Phi_0 R\dot{x}}{D^2(1-x)^3}P_1(\cos\theta) \\
&- \frac{\dot{\Phi}_0 R^2}{D^3(1-x)^3}P_2(\cos\theta) - \frac{3\Phi_0 R^2\dot{x}}{D^3(1-x)^4}P_2(\cos\theta) \\
&+ \frac{\dot{\Phi}_0 R^3}{D^4(1-x)^4}P_3(\cos\theta) + \frac{4\Phi_0 R^3\dot{x}}{D^4(1-x)^5}P_3(\cos\theta) \\
&+ \frac{\dot{\Phi}_1}{D^2(1-x)^2} + \frac{2\Phi_1\dot{x}}{D^2(1-x)^3} + O(h^5)
\end{aligned}$$

at r = R.

Substitution for R from equation (19) and simplification gives

$$-\frac{\partial \Phi}{\partial t} = -\frac{\dot{\Phi}_0}{R_0}\left\{1 - \frac{R_2}{R_0}P_2(\cos\theta) - \frac{R_3}{R_0}P_3(\cos\theta)\right\}$$

$$-\frac{\dot{\Phi}_1}{R_0^2}P_1(\cos\theta) - \frac{\dot{\Phi}_2}{R_0^3}P_2(\cos\theta) - \frac{\dot{\Phi}_3}{R_0^4}P_3(\cos\theta)$$

$$-\frac{\dot{\Phi}_0}{D}\left\{1+x\right\} - \frac{\Phi_0\dot{x}}{D} + \frac{\dot{\Phi}_0 R_0}{D^2}P_1(\cos\theta)$$

$$-\frac{\dot{\Phi}_0 R_0^2}{D^3}P_2(\cos\theta) + \frac{\dot{\Phi}_0 R_0^3}{D^4}P_3(\cos\theta)$$

$$+\frac{\dot{\Phi}_1}{D^2} + O(h^5) \qquad (28)$$

at r = R.

Now $q^2/2 = qr^2/2 + q_o^2/2$. Therefore, from equations (21), (22), (27), and 3:2(3)

$$\frac{1}{2}q^2 = \frac{1}{2}\frac{\Phi_0^2}{R_0^4} + \frac{\Phi_0}{R_0^2}\left\{\dot{R}_2 P_2(\cos\theta) + \dot{R}_3 P_3(\cos\theta)\right\}$$

$$+\frac{9}{2}\frac{\Phi_1^2}{R_0^6}\left\{\frac{2}{3} - \frac{2}{3}P_2(\cos\theta)\right\} + O(h^5)$$

at r = R.

From equation (23)

$$\frac{1}{2}V_0^2 = \frac{1}{2}\left\{\frac{2\Phi_1}{R_0^3} + \frac{\Phi_0}{D^2}\right\}^2 + O(h^5)$$

Substitution of these expressions into equation 3:3(8) gives the following equations to solve:

$$-\frac{\dot{\Phi}_0}{R_0} - \frac{\dot{\Phi}_0}{D}\left\{1+x\right\} - \frac{\Phi_0 \dot{x}}{D} + \frac{\dot{\Phi}_1}{D^2} + \frac{1}{2}\frac{\dot{\Phi}_0^2}{R_0^4} + 3\frac{\Phi_1^2}{R_0^6} =$$

$$1 + \frac{1}{2}\left\{\frac{2\Phi_1}{R_0^3} + \frac{\Phi_0}{D^2}\right\}^2 + O(h^5), \tag{28}$$

$$-\frac{\dot{\Phi}_1}{R_0^2} + \frac{\dot{\Phi}_0 R_0}{D^2} = 0 + O(h^5), \tag{29}$$

$$\frac{\dot{\Phi}_0 R_2}{R_0^2} - \frac{\dot{\Phi}_2}{R_0^3} - \frac{\dot{\Phi}_0 R_0^2}{D^3} + \frac{\Phi_0 \dot{R}_2}{R_0^2} - \frac{3\Phi_1^2}{R_0^6} = 0 + O(h^5), \tag{30}$$

$$\frac{\dot{\Phi}_0 R_3}{R_0^2} - \frac{\dot{\Phi}_3}{R_0^3} + \frac{\dot{\Phi}_0 R_0^3}{D^4} + \frac{\Phi_0 \dot{R}_3}{R_0^2} = 0 + O(h^5). \tag{31}$$

Since it is more convenient to use R_0 as the independent variable, the transformation is made with the use of equation (24) so that

$$\frac{d}{dt} = \dot{R}_0 \frac{d}{dR_0} = \frac{\Phi_0}{R_0^2}\frac{d}{dR_0} + O(h^5).$$

Then equation (25) gives

$$\frac{\Phi_0}{R_0^2}\frac{dR_2}{dR_0} = \frac{-2\Phi_0 R_2}{R_0^3} + \frac{3\Phi_2}{R_0^4} - \frac{2\Phi_0 R_0}{D^3} + O(h^5); \tag{32}$$

equation (26) gives

$$\frac{\Phi_0}{R_0^2}\frac{dR_3}{dR_0} = -\frac{2\Phi_0 R_3}{R_0^3} + \frac{4\Phi_3}{R_0^5} + \frac{3\Phi_0 R_0^2}{D^4} + O(h^5); \tag{33}$$

equation (28) gives

$$-\frac{\Phi_0}{R_0^3}\frac{d\Phi_0}{dR_0} - \frac{\Phi_0(1+x)}{R_0^2 D}\frac{d\Phi_0}{dR_0} - \frac{\Phi_0^2}{R_0^2 D}\frac{dx}{dR_0} + \frac{\Phi_0}{R_0^2 D}\frac{d\Phi_1}{dR_0}$$

$$+\frac{1}{2}\frac{\Phi_0^2}{R_0^4} + \frac{3\Phi_1^2}{R_0^6} = 1 + \frac{1}{2}\left\{\frac{2\Phi_1}{R_0^3} + \frac{\Phi_0}{D^2}\right\}^2 + O(h^5); \tag{34}$$

equation (29) gives

$$-\frac{1}{R_0^2}\frac{d\Phi_1}{dR_0} + \frac{R_0}{D^2}\frac{d\Phi_0}{dR_0} = 0 + O(h^5); \tag{35}$$

equation (30) gives

$$\frac{\Phi_0 R_2}{R_0^4}\frac{d\Phi_0}{dR_0} - \frac{\Phi_0}{R_0^5}\frac{d\Phi_2}{dR_0} - \frac{\Phi_0}{D^3}\frac{d\Phi_0}{dR_0} + \frac{\Phi_0^2}{R_0^4}\frac{dR_2}{dR_0}$$

$$-\frac{3\Phi_1^2}{R_0^6} = 0 + O(h^5); \tag{36}$$

and equation (31) gives

$$\frac{\Phi_0 R_3}{R_0^4}\frac{d\Phi_0}{dR_0} - \frac{\Phi_0}{R_0^5}\frac{d\Phi_3}{dR_0} + \frac{\Phi_0 R_0}{D^4}\frac{d\Phi_0}{dR_0}$$

$$+\frac{\Phi_0^2}{R_0^5}\frac{dR_3}{dR_0} = 0 + O(h^5). \tag{37}$$

To find the solutions as functions of the distance from the wall, the expressions for the unknowns, from equation (8), are substituted into equations (32) through (37). When these equations are solved according to powers of h, the following equations result:

The h^0 terms of equation (34) give

$$-\frac{\Phi_0^{(0)}}{R_0^3}\frac{d\Phi^{(0)}}{dR_0}+\frac{1}{2}\left\{\frac{\Phi_0^{(0)}}{R_0^2}\right\}^2=1. \tag{38}$$

The h^1 terms of equation (34) give

$$-\frac{\Phi_0^{(1)}}{R_0^3}\frac{d\Phi_0^{(0)}}{dR_0}-\frac{\Phi_0^{(0)}}{R_0^3}\frac{d\Phi_0^{(1)}}{dR_0}-\frac{\Phi_0^{(0)}}{R_0^2}\frac{d\Phi_0^{(0)}}{dR_0}+\frac{\Phi_0^{(1)}\Phi_0^{(0)}}{R_0^4}=0. \tag{39}$$

The h^2 terms of equation (34) give

$$-\frac{\Phi_0^{(0)}}{R_0^3}\frac{d\Phi_0^{(2)}}{dR_0}-\frac{\Phi_0^{(1)}}{R_0^3}\frac{d\Phi_0^{(1)}}{dR_0}-\frac{\Phi_0^{(2)}}{R_0^3}\frac{d\Phi_0^{(0)}}{dR_0}-\frac{\Phi_0^{(0)}}{R_0^2}\frac{d\Phi_0^{(1)}}{dR_0}$$

$$-\frac{\Phi_0^{(1)}}{R_0^2}\frac{d\Phi_0^{(0)}}{dR_0}+\frac{1}{2}\left\{\frac{\Phi_0^{(1)}}{R_0^2}\right\}^2+\frac{\Phi_0^{(0)}\Phi_0^{(2)}}{R_0^4}=0. \tag{40}$$

The h^3 terms of equation (34) give

$$-\frac{\Phi_0^{(0)}}{R_0^3}\frac{d\Phi_0^{(3)}}{dR_0}-\frac{\Phi_0^{(1)}}{R_0^3}\frac{d\Phi_0^{(2)}}{dR_0}-\frac{\Phi_0^{(2)}}{R_0^3}\frac{d\Phi_0^{(1)}}{dR_0}-\frac{\Phi_0^{(3)}}{R_0^3}\frac{d\Phi_0^{(0)}}{dR_0}$$

$$-\frac{\Phi_0^{(0)}}{R_0^2}\frac{d\Phi_0^{(2)}}{dR_0}-\frac{\Phi_0^{(1)}}{R_0^2}\frac{d\Phi_0^{(1)}}{dR_0}-\frac{\Phi_0^{(2)}}{R_0^2}\frac{d\Phi_0^{(0)}}{dR_0}$$

$$+\frac{\Phi_0^{(0)}\Phi_0^{(3)}}{R_0^4}+\frac{\Phi_0^{(1)}\Phi_0^{(2)}}{R_0^4}=0. \tag{41}$$

The h^2 terms of equation (35) give

$$\frac{d\Phi_1^{(2)}}{dR_0} = R_0^3 \frac{d\Phi_0^{(0)}}{dR_0} \tag{42}$$

The h^3 terms of equation (35) give

$$\frac{d\Phi_1^{(3)}}{dR_0} = R_0^3 \frac{d\Phi_0^{(1)}}{dR_0}. \tag{43}$$

The h^4 terms of equation (35) give

$$\frac{d\Phi_1^{(4)}}{dR_0} = R_0^3 \frac{d\Phi_0^{(2)}}{dR_0}. \tag{44}$$

The h^3 terms of equation (36) give

$$\frac{d\Phi_2^{(3)}}{dR_0} = R_0 R_2^{(3)} \frac{d\Phi_0^{(0)}}{dR_0} - R_0^5 \frac{d\Phi_0^{(0)}}{dR_0} + \Phi_0^{(0)} R_0 \frac{dR_2^{(3)}}{dR_0}. \tag{45}$$

The h^4 terms of equation (36) give

$$\frac{d\Phi_2^{(4)}}{dR_0} = R_0 R_2^{(4)} \frac{d\Phi_0^{(0)}}{dR_0} + R_0 R_2^{(3)} \frac{d\Phi_0^{(1)}}{dR_0} - R_0^5 \frac{d\Phi_0^{(1)}}{dR_0} + \Phi_0^{(0)} R_0 \frac{dR_2^{(4)}}{dR_0} + \Phi_0^{(1)} R_0 \frac{dR_2^{(3)}}{dR_0} - \frac{3\{\Phi_1^{(2)}\}^2}{\Phi_0^{(0)} R_0}. \tag{46}$$

The h^4 terms of equation (37) give

$$\frac{d\Phi_3^{(4)}}{dR_0} = R_0^2 R_3^{(4)} \frac{d\Phi_0^{(0)}}{dR_0} + R^7 \frac{d\Phi_0^{(0)}}{dR_0} + \Phi_0^{(0)} R_0^2 \frac{dR_3^{(4)}}{dR_0}. \tag{47}$$

The h^3 terms of equation (32) give

$$\frac{dR_2^{(3)}}{dR_0} = -\frac{2R_2^{(3)}}{R_0} + \frac{3\Phi_2^{(3)}}{R_0^2\Phi_0^{(0)}} - 2R_0^3. \tag{48}$$

The h^4 terms of equation (32) give

$$\frac{dR_2^{(4)}}{dR_0} = -\frac{2R_2^{(4)}}{R_0} + \frac{3}{R_0^2}\left[\frac{\Phi_2^{(4)}}{\Phi_0^{(0)}} - \frac{\Phi_0^{(1)}\Phi_2^{(3)}}{\{\Phi_0^{(0)}\}^2}\right]. \tag{49}$$

The h^4 terms of equation (33) give

$$\frac{dR_3^{(4)}}{dR_0} = \frac{-2R_3^{(4)}}{R_0} + \frac{4\Phi_3^{(4)}}{R_0^3\Phi_0^{(0)}} + 3R_0^4. \tag{50}$$

Since $(D/2)(1-X)$ is the distance from the bubble origin to the wall,

$$V_0 = \frac{d}{dt}\,\frac{D(1-X)}{2} = -D\dot{X}/2,$$

or, using equation (23) and multiplying through $2/D$,

$$-\frac{\Phi_0}{R_0^2}\dot{X} = \frac{2}{D}\left\{\frac{2\Phi_1}{R_0^3} + \frac{\Phi_0}{D^2}\right\}.$$

Substituting for X from equation (8), one obtains

$$\frac{dX^{(3)}}{dR_0} = -\frac{4\Phi_1^{(2)}}{R_0\Phi_0^{(0)}} - 2R_0^2, \tag{51}$$

$$\frac{dX^{(4)}}{dR_0} = -\frac{\Phi_0^{(1)}}{\Phi_0^{(0)}}\frac{dX^{(3)}}{dR_0} - \frac{4\Phi_1^{(3)}}{R_0\Phi_0^{(0)}} - \frac{2\Phi_0^{(1)}R_0^2}{\Phi_0^{(0)}}, \tag{52}$$

$$\frac{dX^{(5)}}{dR_0} = -\frac{\Phi_0^{(2)}}{\Phi_0^{(0)}}\frac{dX^{(3)}}{dR_0} - \frac{\Phi_0^{(1)}}{\Phi_0^{(0)}}\frac{dX^{(4)}}{dR_0} - \frac{4\Phi_1^{(4)}}{R_0\Phi_0^{(0)}} - \frac{2\Phi_0^{(2)}R_0^2}{\Phi_0^{(0)}}. \tag{53}$$

Equations (38), (39), (40), and (41) can be integrated exactly, starting with (38) and using the results from the preceding solutions for each succeeding equation. The results are

$$\Phi_0^{(0)} = -\sqrt{\tfrac{2}{3}R_0(1-R_0^3)}, \tag{54}$$

$$\Phi_0^{(1)} = -\frac{1}{2}R_0\,\Phi_0^{(0)}, \tag{55}$$

as before, and

$$\Phi_0^{(2)} = \frac{3}{8}R_0^2\,\Phi_0^{(0)}, \tag{56}$$

$$\Phi_0^{(3)} = -\frac{5}{16}R_0^3\,\Phi_0^{(0)}, \tag{57}$$

Equations (42) through (53) have been integrated numerically by Milne's method [19]. Equations (42), (43), and (44) are integrated separately from the above results. Then the pairs of equations (45) and (48), (46) and (49), (47) and (50) are integrated simultaneously, again using the results from the preceding solutions. Finally equations (51), (52), and (53) are separately integrated.

The results of these integrations are shown in Table 1.

The pressure field is calculated from equation 3:3(6) applied at the point of interest. This gives

$$p = 1 + \frac{\partial\Phi}{\partial t} + \frac{1}{2}(V_0^2 - q^2). \tag{58}$$

The terms in this equation are calculated as before and then, by expanding p in powers of h as in equation (8)

$$p = \sum_{m=0}^{\infty} h^m p^m(r, \theta, R_o), \tag{8'''}$$

the coefficients $p^{(m)}(r, 0, R_o)$ can be found as functions of r, 0, and R_o. The results of this calculation are, for r D(1-X),

$$p^{(0)} = 1 + \frac{1}{r}\frac{\Phi_o^{(0)}}{R_o^2}\frac{d\Phi_o^{(0)}}{dR_o} - \frac{1}{2}\frac{\{\Phi_o^{(0)}\}^2}{r^4},$$

$$p^{(1)} = \frac{1}{r}\left\{\frac{\Phi_o^{(0)}}{R_o^2}\frac{d\Phi_o^{(1)}}{dR_o} + \frac{\Phi_o^{(1)}}{R_o^2}\frac{d\Phi_o^{(0)}}{dR_o}\right\} + \frac{\Phi_o^{(0)}}{R_o^2}\frac{d\Phi_o^{(0)}}{dR_o} - \frac{\Phi_o^{(0)}\Phi_o^{(1)}}{r^4},$$

$$p^{(2)} = \left\{\frac{\Phi_o^{(0)}}{R_o^2}\frac{d\Phi_o^{(1)}}{dR_o} + \frac{\Phi_o^{(1)}}{R_o^2}\frac{d\Phi_o^{(0)}}{dR_o}\right\} + \frac{1}{r}\left\{\frac{\Phi_o^{(0)}}{R_o^2}\frac{d\Phi_o^{(2)}}{dR_o}\right.$$

$$\left. + \frac{\Phi_o^{(1)}}{R_o^2}\frac{d\Phi_o^{(1)}}{dR_o} + \frac{\Phi_o^{(2)}}{R_o^2}\frac{d\Phi_o^{(0)}}{dR_o}\right\} - \frac{1}{r^4}\left\{\Phi_o^{(0)}\Phi_o^{(2)}\right.$$

$$\left. + \frac{1}{2}\left[\Phi_o^{(1)}\right]^2\right\} + P_1(\cos\theta)\left[-r\frac{\Phi_o^{(0)}}{R_o^2}\frac{d\Phi_o^{(0)}}{dR_o}\right.$$

$$+ \frac{1}{r^2}\frac{2\Phi_o^{(0)}\Phi_1^{(2)}}{R_o^3} + \frac{1}{r^2}\frac{\Phi_o^{(0)}}{R_o^2}\frac{d\Phi_1^{(2)}}{dR_o} - \frac{2\Phi_o^{(0)}\Phi_1^{(2)}}{r^5},$$

$$p^{(3)} = \left\{ \frac{\Phi_0^{(0)}}{R_0^2} \frac{d\Phi_0^{(2)}}{dR_0} + \frac{\Phi_0^{(1)}}{R_0^2} \frac{d\Phi_0^{(1)}}{dR_0} + \frac{\Phi_0^{(2)}}{R_0^2} \frac{d\Phi_0^{(0)}}{dR_0} \right\}$$

$$+ \frac{1}{r} \left\{ \frac{\Phi_0^{(0)}}{R_0^2} \frac{d\Phi_0^{(3)}}{dR_0} + \frac{\Phi_0^{(1)}}{R_0^2} \frac{d\Phi_0^{(2)}}{dR_0} + \frac{\Phi_0^{(2)}}{R_0^2} \frac{d\Phi_0^{(1)}}{dR_0} \right.$$

$$\left. + \frac{\Phi_0^{(3)}}{R_0^2} \frac{d\Phi_0^{(0)}}{dR_0} \right\} - \frac{1}{r^4} \left\{ \Phi_0^{(0)} \Phi_0^{(3)} + \Phi_0^{(1)} \Phi_0^{(2)} \right\}$$

$$+ P_1(\cos\theta) \left[-r \left\{ \frac{\Phi_0^{(0)}}{R_0^2} \frac{d\Phi_0^{(1)}}{dR_0} + \frac{\Phi_0^{(1)}}{R_0^2} \frac{d\Phi_0^{(0)}}{dR_0} \right\} \right.$$

$$+ \frac{1}{r^2} \left\{ \frac{2\Phi_0^{(0)} \Phi_1^{(3)}}{R_0^3} + \frac{2\Phi_0^{(1)} \Phi_1^{(2)}}{R_0^3} \right\}$$

$$+ \frac{1}{r^2} \left\{ \frac{\Phi_0^{(1)}}{R_0^2} \frac{d\Phi_1^{(2)}}{dR_0} + \frac{\Phi_0^{(0)}}{R_0^2} \frac{d\Phi_1^{(3)}}{dR_0} \right\}$$

$$\left. - \frac{1}{r^5} \left\{ 2\Phi_0^{(0)} \Phi_1^{(3)} + 2\Phi_0^{(1)} \Phi_1^{(2)} \right\} \right]$$

$$+ P_2(\cos\theta) \left[r^2 \frac{\Phi_0^{(0)}}{R_0^{(2)}} \frac{d\Phi_0^{(0)}}{dR_0} + \frac{2}{r} \left\{ \Phi_0^{(0)} \right\}^2 \right]$$

$$+ P_2(\cos\theta) \left[\frac{1}{r^3} \frac{\Phi_0^{(0)}}{R_0^2} \frac{d\Phi_2^{(3)}}{dR_0} - \frac{1}{r^6} 3\Phi_0^{(0)} \Phi_2^{(3)} \right].$$

The time of collapse τ can be found by integrating equation (24) with the aid of equations (54), (55), (56), and (57). Inverting equation (24), one gets

$$\frac{dt}{dR_0} = \frac{R_0^2}{\Phi_0} + O(h^5).$$

Now

$$\tau = \int_1^0 \frac{dt}{dR_0} \, dR_0 ,$$

or, from equations (55) and (56),

$$\mathcal{T} = \int_1^0 \frac{R_0^2\, dR_0}{\Phi_0^{(0)}\{1 - hR_0/2 + h^2 3R_0^2/8} + O(h^3).$$

Substitution from equation (54) and integration gives

$$\mathcal{T} = \mathcal{T}^{(0)} + h\mathcal{T}^{(1)} + h^2\mathcal{T}^{(3)} + O(h^3)$$

$$= .915(1 + .41h - .09h^2) + O(h^3).$$

3:6. Discussion of the Results.

The time of collapse for a bubble formed at the wall is found by setting h = 1/2 in the expression for $\mathcal{T}$, giving

$$\mathcal{T} = 1.20\, \mathcal{T}^{(0)}$$

which is 20% longer than the time of collapse calculated from the Rayleigh solution. This completely explains the discrepancy between the experimental and theoretical results found by Plesset [2] and illustrated in Fig. 4.

In Fig. 6 the shape of the bubble initially in contact with the wall, is shown at several stages of the collapse. It is noticed first that the bubble surface does not remain in contact with the wall. This displacement is due to the slow convergence of the series expansion for Φ in the case where h = 1/2. Since the effect of the wall on the motion will be the greatest at the point of contact, the calculated distance from the wall to the bubble surface can be used as a guide to the error in the calculated shape of the bubble. The calculations for this case give valid results down to $R_0 = .5$. At $R_0 = .4$, a dotted figure is added which includes the next higher terms in the approximation. It is seen that the deviation between the two degrees of approximation is quite marked, however judging from the position of the wall, the true shape will be intermediate between the two. Over the range of its validity, the calculated shape agrees very well with the experimental results shown in Fig. 3.

For the case of $h = 1/3$ the bubble stays approximately spherical down to a mean radius of .3 . The shape of the bubble at $R_o = .2$ is shown in Fig. 7d, again for the two different orders of approximation. At this point it is doubtful if the expansions used are valid, but in analogy with the case of $h = 1/2$, if it is assumed that the correct result is intermediate between the two figures, then a shape is found similar to that given in Fig. 8. This figure is given by Cole [20] as the experimentally determined shape of an oscillating gas sphere near its minimum radius when it has translatory motion through the liquid. The shape here is similar because in the later stages of collapse, the main effect of the wall is due to the induced motion of the bubble towards the wall.

Thus it is seen that within the range of their validity, the calculated results explain the observed times and shapes, although the deformation becomes too larg e during the later stages of collapse to apply the method used here for the calculation of the shape of the bubble. Figure 7d does suggest the possibility of a re-entrant jet forming at the top of the bubble, but this can only be in the nature of a speculation.

IV CALCULATION OF COLLAPSE WITH TRANSLATORY MOTION OF THE BUBBLE

4:1 The Coordinate System.

Again the coordinate system is set up with an origin placed in the bubble, but in this case the positive z direction is taken to be the direction of the stream flow at a large distance from the bubble. Polar coordinates are introduced as before, the problem again being ϕ independent, and the radius of the bubble assumed to be

$$R = \sum_{n=0}^{\infty} R_n(t)\, P_n(\cos\theta), \tag{1}$$

where the $R_n(t)$ are functions of time to be determined by the problem. The origin is chosen such that $R_1 = 0$ throughout the motion.

4:2 The Differential Equations.

The solution to this problem consists in the simultaneous solution of the two simpler problems, with their appropriate equations, given in 3:2.

4:3 The Boundary Conditions.

The boundary conditions on the fluid motion are: the pressure must be zero on the bubble surface, and the velocity at an infinite distance from the cavity must be equal to a constant value V in the z direction. These are expressed analytically as follows:

$$p = 0, \qquad at \ r = R; \tag{1}$$

$$\bar{V} = -\nabla\Phi = -\bar{e}_z V \quad at \ r = \infty; \tag{2}$$

where $\bar{e}_z$ is the unit vector in the z direction. Again equation (1) must be expressed as a condition on Φ. The general relation for p is, from equation 3:3(5)

$$-\frac{\partial\Phi}{\partial t} + \frac{1}{2}q^2 = -\frac{p}{\rho} + C(t), \tag{3}$$

where C (t) can be evaluated by letting $r \to \infty$. Since the velocity of the liquid at infinity is $\bar{e}_z V$ and the velocity of the origin is $\bar{e}_z v_o$, it follows that at infinity $\bar{q} = \bar{e}_z(V-v_o)$, and Φ is independent of time. If the pressure at infinity is denoted by P_∞, then equation (3) becomes

$$\frac{1}{2}(V-V_0)^2 = -\frac{P_\infty}{\rho} + C(t),$$

or

$$C(t) = \frac{1}{2}(V-V_0)^2 + \frac{P_\infty}{\rho}.$$

Substitution back into equation (3) gives

$$-\frac{\partial\Phi}{\partial t} + \frac{1}{2}q^2 = \frac{P_\infty - p}{\rho} + \frac{1}{2}(V-V_0)^2. \tag{4}$$

Combining this with equation (1) and setting $P_{\infty}/\rho = 1$ as before, one finds the final result to be

$$-\frac{\partial \Phi}{\partial t} + \frac{1}{2} q^2 = 1 + \frac{1}{2}(V - V_0)^2 \tag{5}$$

at r = R.

4:4 <u>The Initial Conditions.</u>

The cavity is initially a sphere of radius unity at rest with respect to a stationary reference system. The liquid has a velocity V in the z direction at large distances from the cavity.

4:5 <u>The Calculations.</u>

A general solution of equation 3:2(1), valid for the region outside the bubble, and satisfying condition 4:3(2), is given by

$$\Phi = \sum_{n=0}^{\infty} \frac{\Phi_n(t)}{r^{n+1}} P_n(\cos\theta) - Vr\cos\theta, \tag{1}$$

where the $\Phi_n(t)$ are functions of time only, to be determined by the problem in a manner similar to that used in Part III.

The procedure for solution is then to substitute expressions 4:1(1) and 4:5(1) for R and Φ into equations 3:2(6) and 4:3(5) which hold at r = R. In this manner two first-order differential equations are obtained, each containing terms in $P_n(\cos\theta)$ which independently satisfy the equations.

It is convenient to introduce a dimensionless parameter k such that $k = \frac{V}{\sqrt{P_{\infty}/\rho}}$. Thus k can be substituted for V in all the equations, since the choice of units to make $P_{\infty}/\rho = 1$

gives k and V the same numerical value.

Now the solutions to the problem must depend on the stream velocity V of the fluid. It is assumed that R_n and $\quad_n$ are functions of k that can be expanded into a Taylor's series about the spherically symmetric case of k = 0, as follows:

$$R_n = \sum_{m=0}^{\infty} k^m R_n^{(m)}(R_0),$$
$$\Phi_n = \sum_{m=0}^{\infty} k^m \Phi_n^{(m)}(R_0), \tag{2}$$

where k is constant for the problem, and $R_n^{(m)}(R_o)$, $\Phi_n^{(m)}(R_o)$ are functions of the mean radius R_o only. Then the coefficients of equal powers of k are equated to give the differential equations for $R_n^{(m)}$ and $\Phi_n^{(m)}$. These are simultaneous first order equations which can be solved in pairs from the initial conditions.

Binomial expansions in terms of $\dfrac{R - R_o}{R_o}$ will be used freely in the following work, under the assumption that the absolute value of this quantity is less than unity. The justification for this assumption will appear from the calculated values of this expression.

The calculations will be done in one step up to terms of $O(k^3)$ since the order of each term can be predicted in advance. Here Φ_1 must be of $O(k)$ to give a fluid velocity at infinity equal to k and yet have the velocity of the bubble initially zero. Thus starting with $P_1(\cos\theta)$, the coefficient of each Legendre polynomial will be of one order less in k than the corresponding one was in h.

Therefore, considering only terms less than $O(k^4)$, the equations are:

Equation (1) takes the form

$$\Phi = -Kr\cos\theta + \frac{\Phi_0}{r} + \frac{\Phi_1}{r^2}P_1(\cos\theta) + \frac{\Phi_2}{r^3}P_2(\cos\theta) + \frac{\Phi_3}{r^4}P_3(\cos\theta) + O(K^4), \tag{3}$$

and equation 4:1(1) the form

$$R = R_0 + R_2 P_2(\cos\theta) + R_3 P_3(\cos\theta) + O(K^4). \tag{4}$$

At r = R, the substitution of equation 3:2(3) in 3:2(6) gives

$$\dot{R} = V_r - V_0\cos\theta - \frac{1}{R}(V_\theta + V_0\sin\theta)\frac{\partial R}{\partial\theta}. \tag{5}$$

From equations (4) and (5)

$$\begin{aligned}\dot{R} &= \dot{R}_0 + \dot{R}_2 P_2(\cos\theta) + \dot{R}_3 P_3(\cos\theta) + O(K^4)\\ &= V_r - V_0\cos\theta - \frac{1}{R}(V_\theta + V_0\sin\theta)\frac{\partial R}{\partial\theta} + O(K^4)\\ &= -\frac{\partial\Phi}{\partial r} - V_0\cos\theta - \frac{1}{R}\left(-\frac{1}{R}\frac{\partial\Phi}{\partial\theta} + V_0\sin\theta\right)\frac{\partial R}{\partial\theta} + O(K^4),\end{aligned} \tag{6}$$

evaluated at r = R. The substitution of equation (3) for Φ and of equation (4) for R in equation (6) gives the following relations, upon equating coefficients of the same Legendre polynomial:

$$\dot{R}_0 = \frac{\Phi_0}{R_0^2} + O(K^4), \tag{7}$$

$$V_0 = k + \frac{2\Phi_1}{R_0^3} + \frac{6}{5}\frac{R_2}{R_0}\frac{\Phi_1}{R_0^3} + O(k^4), \tag{8}$$

$$\dot{R}_2 = -\frac{2\Phi_0 R_2}{R_0^3} + \frac{3\Phi_2}{R_0^4} + O(k^4), \tag{9}$$

$$\dot{R}_3 = -\frac{2\Phi_0 R_3}{R_0^3} - \frac{18}{5}\frac{\Phi_1 R_2}{R_0^4} + \frac{4\Phi_3}{R_0^5}$$

$$-\frac{6}{5}\frac{R_2}{R_0}\left(V_0 - k + \frac{\Phi_1}{R_0^3}\right) + O(k^4). \tag{10}$$

From equations 3:2(2) and 3:2(3) one obtains

$$q_r = -\frac{\partial\Phi}{\partial r} - V_0\cos\theta,$$

and

$$q_\theta = -\frac{1}{r}\frac{\partial\Phi}{\partial\theta} + V_0\sin\theta.$$

Upon substituting for Φ from equation (3) one obtains, at r=R,

$$q_r = \frac{\Phi_0}{R_0^2} + P_1(\cos\theta)\left\{k - V_0 + \frac{2\Phi_1}{R_0^3} - \frac{12}{5}\frac{\Phi_1 R_2}{R_0^4}\right\} + O(k^2), \tag{11}$$

$$q_\theta = P_1(\cos\theta)\left\{-k + V_0 + \frac{\Phi_1}{R_0^3}\right\} + O(k^2). \tag{12}$$

Equation 4:3(5) gives

$$-\frac{\partial\Phi}{\partial t}+\frac{1}{2}q^2=1+\frac{1}{2}(K-V_0)^2$$

at r = R. This equation is to be broken down into its component parts by taking each term, expressing it as a sum of Legendre polynomials and then combining terms according to this equation. From equations (3) and (4)

$$-\frac{\partial\Phi}{\partial t}=-\frac{\dot{\Phi}_0}{R_0}\left\{1-\frac{R_2}{R_0}P_2(\cos\theta)-\frac{R_3}{R_0}P_3(\cos\theta)\right\}$$
$$-\frac{\dot{\Phi}_1}{R_0^2}\left\{P_1(\cos\theta)-\frac{2}{5}\frac{R_2}{R_0}\left[2P_1(\cos\theta)+3P_3(\cos\theta)\right]\right\}$$
$$-\frac{\dot{\Phi}_2}{R_0^3}P_2(\cos\theta)\quad-\frac{\dot{\Phi}_3}{R_0^4}P_3(\cos\theta)+O(K^4).$$

Now $q^2/2=q_r^{\,2}/2+q_\theta^{\,2}/2$. Therefore, using equations (11) and (12) evaluated at r = R, one finds

$$\frac{1}{2}q^2=\frac{1}{2}\frac{\Phi_0^{\,2}}{R_0^4}+\frac{\Phi_0}{R_0^2}\Bigg\{\left(K-V_0+\frac{2\Phi_1}{R_0^3}\right)P_1(\cos\theta)-\frac{12}{5}\frac{\Phi_1R_2}{R_0^4}P_1(\cos\theta)$$
$$-\frac{2\Phi_0R_2}{R_0^3}P_2(\cos\theta)+\frac{3\Phi_2}{R_0^4}P_2(\cos\theta)-\frac{2\Phi_0R_3}{R_0^3}P_3(\cos\theta)$$
$$-\frac{18}{5}\frac{\Phi_1R_2}{R_0^4}P_3(\cos\theta)+\frac{4\Phi_3}{R_0^5}P_3(\cos\theta)\Bigg\}-\frac{2\Phi_0R_2}{R_0^3}\left\{K-V_0+\frac{2\Phi_1}{R_0^3}\right\}$$
$$\left\{\frac{2}{5}P_1(\cos\theta)+\frac{3}{5}P_3(\cos\theta)\right\}+\frac{3\Phi_2}{R_0^4}\left\{K-V_0+\frac{2\Phi_1}{R_0^3}\right\}\left\{\frac{2}{5}P_1(\cos\theta)\right.$$
$$\left.+\frac{3}{5}P_3(\cos\theta)\right\}+\left\{\frac{3\Phi_1}{R_0^3}\right\}^2\left\{\frac{1}{3}-\frac{1}{3}P_2(\cos\theta)\right\}$$
$$+\frac{3\Phi_1\Phi_2}{R_0^7}\left\{\frac{6}{5}P_1(\cos\theta)-\frac{6}{5}P_3(\cos\theta)\right\}+O(K^4).$$

From equation (8)

$$1+\frac{1}{2}(k-V_0^2)=1+\frac{1}{2}\left\{\frac{2\Phi_1}{R_0^3}+\frac{6}{5}\frac{R_2\Phi_1}{R_0^4}\right\}^2+O(k^4).$$

Upon substitution of these expressions back into the equation, one obtains the following equations:

$$-\frac{\dot{\Phi}_0}{R_0}+\frac{1}{2}\frac{\dot{\Phi}_1}{R_0^4}+\frac{3\Phi_1^2}{R_0^6}=1+\frac{2\Phi_1^2}{R_0^6}+O(k^4), \tag{13}$$

$$-\frac{\dot{\Phi}_1}{R_0^2}+\frac{4}{5}\frac{\dot{\Phi}_1R_2}{R_0^3}-\frac{18}{5}\frac{\Phi_0\Phi_1R_2}{R_0^6}+\frac{18}{5}\frac{\Phi_1\Phi_2}{R_0^7}=0+O(k^4), \tag{14}$$

$$-\frac{\dot{\Phi}_2}{R_0^3}+\frac{\dot{\Phi}_0R_2}{R_0^2}-\frac{2\Phi_0^2R_2}{R_0^5}+\frac{3\Phi_0\Phi_2}{R_0^6}$$

$$-\frac{3\Phi_1^2}{R_0^6}=0+O(k^4), \tag{15}$$

$$-\frac{\dot{\Phi}_3}{R_0^4}+\frac{\dot{\Phi}_0R_3}{R_0^2}+\frac{6}{5}\frac{\Phi_1R_2}{R_0^3}-\frac{2\Phi_0^2R_3}{R_0^5}+\frac{4\Phi_0\Phi_3}{R_0^7}$$

$$-\frac{18}{5}\frac{\Phi_0\Phi_1R_2}{R_0^6}-\frac{18}{5}\frac{\Phi_1\Phi_2}{R_0^7}=0+O(k^4). \tag{16}$$

Upon changing the independent variable to R_0 as in Part III, and then substituting in the expressions for R_n and Φ_n from equation (2), one obtains the following equations:

$$-\frac{\Phi_0^{(0)}}{R_0^3}\frac{d\Phi_0^{(0)}}{dR_0}+\frac{1}{2}\frac{\{\Phi_0^{(0)}\}^2}{R_0^4}=1, \tag{17}$$

$$-\frac{\Phi_0^{(0)}}{R_0^3}\frac{d\Phi_0^{(2)}}{dR_0}-\frac{\Phi_0^{(2)}}{R_0^3}\frac{d\Phi_0^{(0)}}{dR_0}+\frac{\Phi_0^{(0)}\Phi_0^{(2)}}{R_0^4}=-\frac{\{\Phi_1^{(1)}\}^2}{R_0^6}, \tag{18}$$

$$-\frac{\Phi_0^{(0)}}{R_0^4}\frac{d\Phi_1^{(1)}}{dR_0}=0, \tag{19}$$

$$-\frac{\Phi_0^{(0)}}{R_0^4}\frac{d\Phi_1^{(3)}}{dR_0}-\frac{18}{5}\frac{\Phi_0^{(0)}\Phi_1^{(1)}R_2^{(2)}}{R_0^6}+\frac{18}{5}\frac{\Phi_1^{(1)}\Phi_2^{(2)}}{R_0^7}=0, \tag{20}$$

$$-\frac{\Phi_0^{(0)}}{R_0^5}\frac{d\Phi_2^{(2)}}{dR_0}+\frac{\Phi_0^{(0)}R_2^{(2)}}{R_0^4}\frac{d\Phi_0^{(0)}}{dR_0}-\frac{2\{\Phi_0^{(0)}\}^2R_2^{(2)}}{R_0^5}$$
$$+\frac{3\Phi_0^{(0)}\Phi_2^{(2)}}{R_0^6}-\frac{3\{\Phi_1^{(1)}\}^2}{R_0^6}=0, \tag{21}$$

$$\frac{\Phi_0^{(0)}}{R_0^2}\frac{dR_2^{(2)}}{dR_0}=\frac{-2\Phi_0^{(0)}R_2^{(2)}}{R_0^3}+\frac{3\Phi_2^{(2)}}{R_0^4}, \tag{22}$$

$$-\frac{\Phi_0^{(0)}}{R_0^6}\frac{d\Phi_3^{(3)}}{dR_0}+\frac{\Phi_0^{(0)}R_3^{(3)}}{R_0^4}\frac{d\Phi_0^{(0)}}{dR_0}-\frac{2\{\Phi_0^{(0)}\}^2R_3^{(3)}}{R_0^5}$$
$$-\frac{18}{5}\frac{\Phi_0^{(0)}\Phi_1^{(1)}R_2^{(2)}}{R_0^6}+\frac{4\Phi_0^{(0)}\Phi_3^{(3)}}{R_0^7}-\frac{18}{5}\frac{\Phi_2^{(2)}\Phi_1^{(1)}}{R_0^7}=0, \tag{23}$$

$$\frac{\Phi_0^{(0)}}{R_0^2}\frac{dR_3^{(3)}}{dR_0}=-\frac{2\Phi_0^{(0)}R_3^{(3)}}{R_0^3}+\frac{4\Phi_3^{(3)}}{R_0^5}-\frac{36}{5}\frac{\Phi_1^{(1)}R_2^{(2)}}{R_0^5}. \tag{24}$$

The equations for $\Phi_0^{(1)}$, $\Phi_1^{(2)}$, and $\Phi_2^{(3)}$ give these quantities as identically zero throughout the motion. Equations (17), (18), and (19) can be integrated directly to give

$$\Phi_0^{(0)}=-\sqrt{2R_0(1-R_0^3)/3},$$

$$\Phi_1^{(1)}=-1/2,$$

$$\Phi_0^{(2)}=-\Phi_0^{(0)}/8R_0^3.$$

The pairs of equations (21) and (22), (23) and (24) are integrated simultaneously by Milne's method (19) using the results from preceding solutions. The results of these integrations are shown in Table 2.

4:6 Discussion of the Results.

Figure 9 shows the shape of a collapsing bubble with translatory motion where it has been assumed that the motion of the bubble relative to the liquid is approximately one-tenth the liquid velocity ($k = 1/10$). This relative velocity is the order of magnitude of that observed in the High Speed Water Tunnel. The shape is seen to be approximately spherical throughout the greater part of the motion, but at $R_o = .3$ a noticeable deformation has appeared. This agrees very well with the experimentally determined shape in Fig. 8. Unfortunately, for smaller mean radii, the higher order approximations have comparable magnitudes and nothing definite can be said about what happens in the later stages of the collapse, although, again, the formation of a re-entrant jet is suggested.

V CALCULATION OF GROWTH IN THE VICINITY OF A WALL

5:1 The Coordinate System.

The coordinate system is the same as that used in Part III. However, here D/2 is not the initial distance to the wall, but is the distance at approximately maximum size. This avoids any indeterminacy in the parameter h.

5:2 The Differential Equations.

The differential equations and their method of solution are identical to those used in Part III.

5:3 The Boundary Conditions.

Boundary conditions 3:3(1), (2), and (3) are also satisfied for the growth of a bubble, but the pressure at infinity is not taken to be a constant. The pressure field is chosen so as to approximate the experimental conditions found in the high speed water tunnel and yet be of a simple form. The pressure is assumed to be

$$\frac{P_\infty}{\rho} = -\frac{4}{3}R_o + \frac{7}{3}R_o^4, \qquad (1)$$

as compared to the experimental pressure given in Fig. 4. This expression for the pressure yields a time rate of change of mean radius R_o that is zero at $R_o = 0$ and $R_o = 1$.

5:4 The Initial Conditions.

The initial conditions are that the fluid velocity is zero, and that the cavity has zero radius. The distance from the wall is unspecified initially, but when the mean radius approaches unity, the distance from the wall becomes D/2. This gives h = 1/D the same meaning as it had in Part III.

5:5 The Calculations.

The substitution of equation 5:3(1) in equation 3:3(7) gives for the condition on Φ, at r = R.

$$-\frac{\partial\Phi}{\partial t}+\frac{1}{2}q^2=-\frac{4}{3}R_o+\frac{7}{3}R_o^4+\frac{1}{2}V_o^2. \tag{1}$$

The only difference between the equations in Part III and Part V is in the h and θ independent terms which give equation (1) instead of equation 3:3(8). Thus, if the same conditions on $|X|$ and $\left|\frac{R-R_o}{R_o}\right|$ are assumed as in Part III, and the same manner of solution pursued, the only change in the final differential equations will be in the one for $\Phi_o^{(o)}$, which will be

$$-\frac{\Phi_o^{(o)}}{R_o^3}\frac{d\Phi_o^{(o)}}{dR_o}+\frac{1}{2}\left\{\frac{\Phi_o^{(o)}}{R_o^2}\right\}^2=-\frac{4}{3}R_o+\frac{7}{3}R_o^4, \tag{2}$$

instead of equation 3:5(38). This equation can be integrated directly. It gives

$$-\frac{1}{2}\frac{1}{R_o^3}\frac{d}{dR_o}\left[\Phi_o^{(o)}\right]^2+\frac{1}{2}\frac{1}{R_o^4}\left\{\Phi_o^{(o)}\right\}^2=-\frac{4}{3}R_o+\frac{7}{3}R_o^4,$$

or

$$-\frac{1}{2}\frac{d}{dR_o}\left[\frac{\{\Phi_o^{(o)}\}^2}{R_o}\right]=-\frac{4}{3}R_o+\frac{7}{3}R_o^4.$$

Multiplication by R_o^2 gives

$$\begin{aligned}-\frac{1}{2}\frac{d}{dR_o}\left[\frac{\{\Phi_o^{(o)}\}^2}{R_o}\right]&=-\frac{4}{3}R_o^3+\frac{7}{3}R_o^6\\&=-\frac{1}{3}\frac{d}{dR_o}R_o^4+\frac{1}{3}\frac{d}{dR_o}R_o^7.\end{aligned}$$

Integration gives

$$-\frac{1}{2}\frac{\{\Phi_o^{(o)}\}^2}{R_o}=-\frac{1}{3}R_o^4+\frac{1}{3}R_o^7 + \text{constant}.$$

"ith the initial conditions and the sign chosen for an expanding bubble, one gets

$$\Phi_o^{(o)}=R_o^2\sqrt{\frac{2}{3}R_o(1-R_o^3)}\,.$$

The remainder of the equations are integrated in the same manner as in Part III. The results are given in Table 3.

5:6 Discussion of the Results.

The purpose of this calculation was to demonstrate that the experimentally determined fact of spherical growth is explained by the theory. Since all the coefficients $R_n^{(m)}$ are less than the corresponding R_o, the deviation from spherical shape during the growth, is too small to be observed experimentally.

VI THE VALIDITY OF THE RESULTS

The question naturally arises as to the validity of the binomial expansions used in the development of the results and to the convergence properties of the derived series. From the calculated results it appears that $\left|\frac{R - R_o}{R_o}\right|$ is not less than unity when R_o becomes sufficiently small. This would make results for smaller values of R_o doubtful. However, in the early stages of the motion the solutions are evidently convergent, for the initial conditions are such that the coefficients of low powers of h are larger than those of higher powers. An analysis will be made here to give an idea of the range of validity of the results.

The first item to consider is the behaviour of the coefficients $R_n^{(s)}$ and $\Phi_n^{(s)}$ when R_o becomes small. It will be assumed that for all $s < \sigma$ these coefficients behave according to the following relations: $R_n^{(s)}/R_o \sim 1/R_o^{\alpha s}$, and $\Phi_n^{(s)}/R_o^{n+1/2} \sim 1/R_o^{\alpha s}$, where $\sim$ denotes that the two terms are asymptotic to one another, except for a constant factor, as R_o becomes small. The value of α is to be determined for the smallest values of s and n exhibiting this behaviour. The proof is by mathematical induction and will consist in showing that $R_n^{(\sigma)}/R_o \sim 1/R_o^{\alpha\sigma}$, and $\Phi_n^{(\sigma)}/R_o^{n+1/2} \sim 1/R_o^{\alpha\sigma}$. Due to the fact that r appears in the numerator of the image terms of Φ, these terms will not give as strong a singularity at $R_o = 0$ for the same power of h as will the other terms, and therefore the image terms are neglected in what follows.

Consider first the equation for the motion of the bubble boundary

$$\dot{R} = \dot{R}_o \frac{dR}{dR_o} = q_r - \frac{1}{R}\frac{\partial R}{\partial \theta} q_\theta$$

at r = R. In the preceding sections this equation was broken down into equations for $\dfrac{d R_n^{(\sigma)}}{d R_o}$ by equating coefficients of

h^{σ} and $P_n(\cos\theta)$.

In this process, at r = R,

$$\dot{R}_o \frac{dR}{dR_o} \quad \text{became} \quad \frac{\Phi_o^{(o)}}{R_o^2}\frac{dR_n^{(\sigma)}}{dR_o} + \sum_{\substack{\text{terms}\\ \text{like}}} \frac{\Phi_m^{(y)}}{R_o^{m+2}}\frac{R_p^{(x)}}{R_o}\frac{R_q^{(u)}}{R_o} \cdots \frac{R_r^{(v)}}{R_o},$$

$$q_r \quad \text{became} \quad \frac{\Phi_n^{(\sigma)}}{R_o^{n+2}} + \sum_{\substack{\text{terms}\\ \text{like}}} \frac{\Phi_m^{(y)}}{R_o^{m+2}}\frac{R_p^{(x)}}{R_o} \cdots \frac{R_q^{(u)}}{R_o},$$

$$\frac{1}{R}\frac{\partial R}{\partial \theta} q_\theta \quad \text{became} \sum_{\substack{\text{terms}\\ \text{like}}} \frac{R_m^{(y)}}{R_o} \cdots \frac{R_p^{(x)}}{R_o}\frac{\Phi_q^{(u)}}{R_o^{q+2}}\frac{R_r^{(v)}}{R_o} \cdots,$$

where $x + y + u + v + \cdots \leq \sigma$

Thus

$$\frac{\Phi_o^{(o)}}{R_o^2}\frac{dR_n^{(\sigma)}}{dR_o} + \frac{\Phi_n^{(\sigma)}}{R_o^{n+2}} \sim \sum_{\substack{\text{terms}\\ \text{like}}} \frac{\Phi_m^{(y)}}{R_o^{m+2}}\frac{R_p^{(x)}}{R_o} \cdots \frac{R_q^{(u)}}{R_o}$$

$$\sim \frac{1}{R_o^{3/2}}\frac{1}{R_o^{\alpha\sigma}}. \qquad (1)$$

The condition for zero pressure on the bubble surface, expressed in terms of Φ, is

$$-\frac{\partial \Phi}{\partial t} + \frac{1}{2}q^2 = 1 + \frac{1}{2}V_o^2$$

at r = R. In the same manner

$$-\frac{\partial \Phi}{\partial t} = \dot{R}_o \frac{\partial \Phi}{\partial R_o}$$

became $\dfrac{\Phi_o^{(0)}}{R_o^2} \dfrac{1}{R_o^{n+1}} \dfrac{d\Phi_n^{(\sigma)}}{dR_o} + \sum\limits_{\substack{\text{terms}\\ \text{like}}} \dfrac{\Phi_m^{(y)}}{R_o^{m+2}} \dfrac{d\Phi_p^{(x)}}{dR_o} \dfrac{1}{R_o^{p+1}} \dfrac{R_q^{(u)}}{R_o} \cdots$,

$\frac{1}{2}q^2$ became $\dfrac{\Phi_o^{(0)}}{R_o^2} \dfrac{\Phi_n^{(\sigma)}}{R_o^{n+2}} + \sum\limits_{\substack{\text{terms}\\ \text{like}}} \dfrac{\Phi_m^{(y)}}{R_o^{m+2}} \dfrac{\Phi_p^{(x)}}{R_o^{p+2}} \dfrac{R_q^{(u)}}{R_o} \cdots \dfrac{R_r^{(v)}}{R_o}$,

where $x + y + u + \cdots + v \leq \sigma$, and $v_o^2 \sim q^2$.

Thus

$$\frac{\Phi_o^{(0)}}{R_o^{n+3}} \frac{d\Phi_n^{(\sigma)}}{dR_o} + \frac{\Phi_o^{(0)} \Phi_n^{(\sigma)}}{R_o^{n+4}} \sim \frac{1}{R_o^3} \frac{1}{R_o^{\alpha\sigma}} . \tag{2}$$

Since from equation 3:5(12)

$$\Phi_o^{(0)} \sim R_o^{1/2}$$

it follows from equation (2) that

$$\frac{\Phi_n^{(\sigma)}}{R_o^{n+1/2}} \sim \frac{1}{R_o^{\alpha\sigma}} , \tag{3}$$

and from equations (1) and (3) that

$$\frac{R_n^{(\sigma)}}{R_o} \sim \frac{1}{R_o^{\alpha\sigma}}\,, \tag{4}$$

which proves the contention.

For the case of motion in the vicinity of a wall, $\Phi_1^{(2)}$ approaches a constant value as R_o approaches zero. Thus, since equation (3) gives

$$\frac{\Phi_1^{(2)}}{R_o^{3/2}} \sim \frac{1}{R_o^{2\alpha}}$$

$\alpha = 3/4.$

For the case with translatory motion of the fluid relative to the bubble, $\Phi_1^{(1)}$ approaches a constant value as R_o approaches zero. By a method similar to the above, one obtains for this case $\alpha = 3/2.$

It is interesting to note that $\left|\frac{R - R_o}{R_o}\right|$ and $\left|\frac{h}{R_o^{\alpha}}\right|$ approach unity at approximately the same point in the collapse process.

REFERENCES

(1) Thoma, D., Die Kavitation bei Wasser Turbinen. Hydraulische Probleme V.D.I., Verlag (1926).

(2) Plesset, M.S., Dynamics of Cavitation Bubbles. Journal of Applied Mechanics (1949), Vol. 16, p. 277.

(3) Parsons, C.A. and Cook, S.S., Investigation into the Causes of Corrosion or Erosion of Propellers. Engineering (1919), Vol. 107, p. 515.

(4) Schneider, A.J.R., Some Compressible Effects in Cavitation Bubble Dynamics, California Institute of Technology Ph.D. Thesis (1949).

(5) de Haller, P., Untersuchungen uber die Kavitation hervorgerufenden Korrosion. Schweizerische Bauzeitung (1933), Vol. 101, p. 274.

(6) Ackeret, J. and de Haller, P., Ueber die Zerstorung von Werkstoffen durch Tropfenschlag und Kavitation. Schweitzerische Bauzeitung. (1936), Vol. 108, p. 105.

(7) Rightmire, B.G., A Study of the Damage Producing Mechanism in Hydraulic Cavitation, Massachusetts Institute of Technology Thesis (1941).

(8) Boetcher, H., Failure of Metals due to Cavitation under Experimental Conditions. Transactions American Society of Mechanical Engineers (1936), Vol. 58, p. 355.

(9) Mousson, J., Pitting Resistance of Metals under Cavitation Conditions. Transactions American Society of Mechanical Engineers (1937), Vol. 59, p. 399.

(10) Stepanoff, A., Cavitation in Pumps. Transactions American Society of Mechanical Engineers (1945), Vol. 67, p. 539.

(11) Knapp, R.T., and Hollander, A., Laboratory Investigations of the Mechanism of Cavitation. Transactions American Society of Mechanical Engineers (1948), Vol. 70, p. 419.

(12) Lord Rayleigh, The Pressure Developed in a Liquid during the Collapse of a Spherical Cavity. Philosophical Magazine (1917), Vol. 34, p. 94.

(13) Besant, W., Hydrostatics and Hydrodynamics. Cambridge (1859).

(14) Osborne, M., The Shock produced by a Collapsing Cavity in Water. Transactions American Society of Mechanical Engineers (1947), Vol. 69, p. 253.

(15) Herring, C., Theory of Pulsations of the Gas Bubble Produced by an Underwater Explosion. National Defense Research Council Report C4-sr20-010, (October 1941).

(16) Van Iterson, F.K.T., Cavitation et Tension Superficielle. Knoiklijke Akad. van Wetenshappen te Amsterdam (1936), Vol. 39, pp. 138 and 330. Abstract Engineering (1936), Vol. 142, p. 95.

(17) Lamb, H., Hydrodynamics. Dover (1945), pp. 12,20.

(18) Smythe, W.R., Static and Dynamic Electricity. McGraw-Hill (1939), p. 134.

(19) Margenau, H. and Murphy, G.M., The Mathematics of Physics and Chemistry. Van Nostrand (1947), p. 472.

(20) Cole, R.H., Underwater Explosions. Princeton (1948), p. 279.

TABLE 1

VALUE OF COEFFICIENTS AS A FUNCTION OF THE MEAN RADIUS FOR BUBBLE COLLAPSE IN THE VICINITY OF A WALL

R_0	$R_2^{(3)}$	$R_2^{(4)}$	$R_2^{(5)}$	$R_2^{(6)}$	$R_3^{(4)}$	$R_3^{(5)}$
1.0	0	0	0	0	0	0
0.9	.453	-.0336	9.93×10^{-4}	-.795	-.591	.135
0.8	.821	-.154	1.107×10^{-2}	-.433	-.990	.527
0.7	1.117	-.406	.0452	.621	-1.219	1.181
0.6	1.345	-.869	.127	2.199	-1.283	2.112
0.5	1.497	-1.706	.327	4.208	-1.155	3.247
0.4	1.540	-3.281	.799	6.342	-.774	4.187
0.3	1.388	-6.610	2.097	6.760	-.0310	2.976
0.2	.803	-15.64	6.724	.454	1.178	-8.122
0.1	-	-	-	-	-	-
0.0	-	-	-	-	-	-

R_0	$R_3^{(6)}$	$R_4^{(5)}$	$R_4^{(6)}$	$R_5^{(6)}$	$X^{(3)}$	$X^{(4)}$
1.0	0	0	0	0	0	0
0.9	-6.75×10^{-3}	.701	-.145	-.803	.583	-5.68×10^{-4}
0.8	-.132	1.082	-.479	-1.130	1.143	-4.95×10^{-3}
0.7	-.605	1.194	-.897	-1.091	1.702	-1.96×10^{-2}
0.6	-1.922	1.053	-1.072	-.735	2.290	-4.89×10^{-2}
0.5	-4.955	.644	-.311	-.0813	2.954	-.106
0.4	-13.96	-.0716	3.287	.742	3.770	-.214
0.3	-43.25	-.948	14.44	1.473	4.894	-.331
0.2	-181.8	-1.138	80.90	-	6.715	-.535
0.1	-	-	-	-	10.784	-
0.0	-	-	-	-	-	-

TABLE 1 (Cont'd)

VALUE OF COEFFICIENTS AS A FUNCTION OF THE MEAN RADIUS FOR BUBBLE COLLAPSE IN THE VICINITY OF A WALL

R_o	$X^{(5)}$	$\Phi_0^{(0)}$	$\Phi_0^{(1)}$	$\Phi_0^{(2)}$	$\Phi_0^{(3)}$	$\Phi_1^{(2)}$
1.0	0	0	0	0	0	0
0.9	3.77×10^{-4}	-.403	.181	-.122	.0917	-.369
0.8	4.09×10^{-3}	-.510	.204	-.122	.0816	-.436
0.7	1.45×10^{-2}	-.554	.194	-.102	.0594	-.455
0.6	3.79×10^{-2}	-.560	.168	-.0756	.0377	-.457
0.5	8.16×10^{-2}	-.540	.135	-.0506	.0211	-.454
0.4	.159	-.500	.0999	-.0300	9.99×10^{-3}	-.450
0.3	.300	-.441	.0662	-.0149	2.82×10^{-3}	-.448
0.2	.581	-.364	.0363	-5.46×10^{-3}	9.09×10^{-4}	-.447
0.1	-	-.258	.0129	-9.66×10^{-4}	8.06×10^{-5}	-.446
0.0	-	0	0	0	0	-.446

R_o	$\Phi_1^{(3)}$	$\Phi_1^{(4)}$	$\Phi_2^{(3)}$	$\Phi_2^{(4)}$	$\Phi_2^{(5)}$	$\Phi_2^{(6)}$
1.0	0	0	0	0	0	0
0.9	.167	-.114	.176	-.150	.0894	.0209
0.8	.182	-.115	.0251	-.160	.0826	.495
0.7	.178	-.106	-.114	-.163	.0834	.394
0.6	.171	-.0988	-.201	-.157	.0923	-.0521
0.5	.166	-.0946	-.233	-.137	.105	-.585
0.4	.163	-.0927	-.217	-.101	.104	-1.096
0.3	.161	-.0920	-.163	-.0522	.0986	-1.316
0.2	.161	-.0918	-.0852	-2.55×10^{-3}	.0933	-1.005
0.1	.161	-.0916	-	-	-	-
0.0	.161	-.0916	-	-	-	-

TABLE 1 (Cont'd)

VALUE OF COEFFICIENTS AS A FUNCTION OF THE MEAN RADIUS FOR BUBBLE COLLAPSE IN THE VICINITY OF A WALL

R_o	$\Phi_3^{(4)}$	$\Phi_3^{(5)}$	$\Phi_3^{(6)}$	$\Phi_4^{(5)}$	$\Phi_4^{(6)}$	$\Phi_5^{(6)}$
1.0	0	0	0	0	0	0
0.9	-.118	-.0455	3.43×10^{-3}	.0751	.241	-.0393
0.8	.0382	-.278	.0787	-.0657	.413	.0769
0.7	.129	-.470	.143	-.111	.392	.0867
0.6	.149	-.604	.243	-.0925	.297	.0537
0.5	.122	-.670	.360	-.0530	.180	.0200
0.4	.0747	-.647	.640	-.0180	.0665	2.35×10^{-3}
0.3	.0294	-.509	1.122	-4.95×10^{-3}	-.0453	1.32×10^{-3}
0.2	1.35×10^{-3}	-.282	1.798	5.55×10^{-3}	-.151	-
0.1	-	-	-	-	-	-
0.0	-	-	-	-	-	-

R_o	$dx^{(3)}/dR_o$	$dx^{(4)}/dR_o$	$dx^{(5)}/dR_o$	$\frac{d\Phi_o^{(0)}}{dR_o}$	$\frac{d\Phi_o^{(1)}}{dR_o}$	$\frac{d\Phi_o^{(2)}}{dR_o}$
1.0	-6	0	0	∞	$-\infty$	∞
0.9	-5.68	.0183	-.0159	1.584	-.511	.209
0.8	-5.55	.0771	-.0663	.685	-.0188	-.142
0.7	-5.68	.196	-.162	.224	.198	-.250
0.6	-6.16	.406	-.319	-.0810	.304	-.263
0.5	-7.23	.778	-.576	-.309	.347	-.231
0.4	-9.34	1.456	-1.023	-.496	.349	-.180
0.3	-13.72	2.848	-1.896	-.674	.322	-.122
0.2	-24.64	6.392	-4.041	-.887	.271	-.068
0.1	-69.19	-	-	-1.286	.193	-.024
0.0	-	-	-	$-\infty$	0	0

TABLE 1 (Cont'd)

VALUE OF COEFFICIENTS AS A FUNCTION OF THE MEAN RADIUS FOR BUBBLE COLLAPSE IN THE VICINITY OF A WALL

R_o	$\frac{d\Phi_0^{(3)}}{dR_o}$	$\frac{d\Phi_1^{(2)}}{dR_o}$	$\frac{d\Phi_1^{(3)}}{dR_o}$	$\frac{d\Phi_1^{(4)}}{dR_o}$	$\frac{d\Phi_2^{(3)}}{dR_o}$	$\frac{d\Phi_2^{(4)}}{dR_o}$
1.0	$-\infty$	$+\infty$	$-\infty$	∞	$-\infty$	∞
0.9	-.055	1.155	-.374	.152	1.192	.240
0.8	.196	.351	-9.61×10^{-3}	-.0727	1.576	.0456
0.7	.231	.0768	.0680	-.0856	1.151	-.0101
0.6	.194	-.0175	.0657	-.0568	.586	-.120
0.5	.138	-.0386	.0434	-.0289	.0663	-.283
0.4	.0848	-.0318	.0223	-.0115	-.364	-.438
0.3	.0429	-.0182	8.35×10^{-3}	-3.30×10^{-3}	-.681	-.524
0.2	.0158	-7.10×10^{-3}	2.17×10^{-3}	-5.44×10^{-4}	-.835	-.430
0.1	.0028	-1.29×10^{-3}	1.93×10^{-4}	-2.4×10^{-5}	-	-
0.0	0	0	0	0	-	-

R_o	$\frac{d\Phi_2^{(5)}}{dR_o}$	$\frac{d\Phi_2^{(6)}}{dR_o}$	$\frac{d\Phi_3^{(4)}}{dR_o}$	$\frac{d\Phi_3^{(5)}}{dR_o}$	$\frac{d\Phi_3^{(6)}}{dR_o}$	$\frac{d\Phi_4^{(5)}}{dR_o}$
1.0	$-\infty$	∞	∞	$-\infty$	∞	$-\infty$
0.9	.0241	-7.859	-1.599	2.320	-.880	1.766
0.8	.0367	-1.306	-1.308	2.173	-.644	.926
0.7	-.0718	3.169	- .518	1.577	-.781	.0690
0.6	-.158	5.374	.0852	1.009	-1.310	-.326
0.5	-.0501	5.458	.411	.216	-2.483	-.372
0.4	7.63×10^{-3}	4.354	.492	-.786	-3.811	-.233
0.3	.0340	-.974	.385	-1.913	-5.143	-.140
0.2	.176	-3.137	.179	-3.355	-10.02	.114
0.1	-	-	-	-	-	-
0.0	-	-	-	-	-	-

TABLE 1 (Cont'd)

VALUE OF COEFFICIENTS AS A FUNCTION OF THE MEAN RADIUS FOR BUBBLE COLLAPSE IN THE VICINITY OF A WALL

R_o	$\frac{d\Phi_4^{(6)}}{dR_o}$	$\frac{d\Phi_5^{(6)}}{dR_o}$
1.0	∞	∞
0.9	-3.037	-1.774
0.8	-.498	-.546
0.7	.794	.196
0.6	1.266	.349
0.5	1.357	.228
0.4	1.252	.0729
0.3	.425	.0535
0.2	-	-
0.1	-	-
0.0	-	-

TABLE 2

VALUE OF COEFFICIENTS AS A FUNCTION OF THE MEAN RADIUS FOR BUBBLE COLLAPSE WITH INITIAL TRANSLATORY MOTION OF THE LIQUID

R_0	$R_2^{(2)}$	$R_3^{(3)}$	$\Phi_0^{(0)}$	$\Phi_0^{(2)}$	$\Phi_1^{(3)}$	$\Phi_2^{(2)}$
1.0	0	0	0	0	0	0
0.9	-.248	-.235	-.403	.0691	.170	-.259
0.8	-.588	-.840	-.510	.124	.447	-.278
0.7	-1.068	-2.021	-.554	.202	.929	-.249
0.6	-1.778	-4.353	-.560	.324	1.798	-.190
0.5	-2.901	-9.100	-.540	.540	3.51	-.124
0.4	-4.861	-21.05	-.500	.976	7.29	-.0681
0.3	-8.973	-57.92	-.441	2.040	19.77	-.0062
0.2	-20.37	-250	-.364	5.69	63.2	.0295
0.1	-92.75	-1000	-.258	32.3	666	.160
0.0	-	-	0	∞	-	-

$$\Phi_0^{(1)} = \Phi_1^{(2)} = \Phi_2^{(3)} = 0$$

$$\Phi_1^{(1)} = -\frac{1}{2}$$

R_0	$\Phi_3^{(3)}$	$\frac{dR_2^{(2)}}{dR_0}$	$\frac{dR_3^{(3)}}{dR_0}$	$\frac{d\Phi_0^{(0)}}{dR_0}$	$\frac{d\Phi_0^{(2)}}{dR_0}$	$\frac{d\Phi_1^{(3)}}{dR_0}$
1.0	0	2.25	0	∞	$-\infty$	-1.35
0.9	-.0563	2.93	4.04	1.58	-.501	-2.14
0.8	.0136	4.05	8.38	.685	-.632	-3.57
0.7	.178	5.81	16.2	.224	-.947	-6.28
0.6	.418	8.82	32.5	-.0810	-1.573	-11.72
0.5	.701	14.5	61.8	-.309	-2.851	-24.20
0.4	1.096	26.9	187	-.496	-6.35	-56.5
0.3	1.624	60.3	655	-.674	-17.28	-181
0.2	2.50	198	4100	-.887	-71.4	-899
0.1	5.0	1670	-	-1.286	-808	-15,600
0.0	-	-	-	$-\infty$	$-\infty$	-

TABLE 2 (Cont'd)

VALUE OF COEFFICIENTS AS A FUNCTION OF THE MEAN RADIUS FOR BUBBLE COLLAPSE WITH INITIAL TRANSLATORY MOTION OF THE LIQUID

R_o	$\frac{d\Phi_2^{(2)}}{dR_o}$	$\frac{d\Phi_3^{(3)}}{dR_o}$
1.0	∞	1.35
0.9	.650	-.124
0.8	-.135	-1.22
0.7	-.482	-2.06
0.6	-.644	-2.73
0.5	-.690	-3.58
0.4	-.638	-4.48
0.3	-.489	-6.30
0.2	-.338	-14
0.1	-	-
0.0	-	-

TABLE 3

VALUE OF COEFFICIENTS AS A FUNCTION OF THE MEAN RADIUS FOR BUBBLE GROWTH IN THE VICINITY OF A WALL

R_0	$R_2^{(3)}$	$R_3^{(4)}$	$X^{(3)}$	$\Phi_0^{(0)}$	$\Phi_0^{(1)}$	$\Phi_1^{(2)}$
0.0	0	0	1.0	0	0	0
0.1	-8.83×10^{-5}	8.37×10^{-6}	.999	2.58×10^{-3}	-1.29×10^{-4}	1.17×10^{-6}
0.2	-1.41×10^{-3}	2.68×10^{-4}	.990	1.46×10^{-2}	-1.46×10^{-3}	5.31×10^{-5}
0.3	-7.14×10^{-2}	2.04×10^{-3}	.966	3.97×10^{-2}	-5.95×10^{-3}	4.87×10^{-4}
0.4	-2.22×10^{-2}	8.60×10^{-3}	.919	8.00×10^{-2}	-1.60×10^{-2}	2.29×10^{-3}
0.5	-5.28×10^{-2}	2.61×10^{-2}	.843	1.35×10^{-1}	-3.37×10^{-2}	7.45×10^{-3}
0.6	-.105	7.10×10^{-2}	.729	2.01×10^{-1}	-6.03×10^{-2}	1.86×10^{-2}
0.7	-.194	.159	.574	2.71×10^{-1}	-9.48×10^{-2}	3.78×10^{-2}
0.8	-.330	.315	.374	3.37×10^{-1}	-1.35×10^{-1}	6.04×10^{-2}
0.9	-.504	.556	.144	3.26×10^{-1}	-1.45×10^{-1}	5.77×10^{-2}
1.0	(-.735)	(.995)	(0)	0	0	-

R_0	$\Phi_2^{(3)}$	$\Phi_3^{(4)}$	$\frac{dX^{(3)}}{dR_0}$	$\frac{d\Phi_0^{(0)}}{dR_0}$	$\frac{d\Phi_0^{(1)}}{dR_0}$	$\frac{d\Phi_1^{(2)}}{dR_0}$
0.0	0	0	0	0	0	0
0.1	-2.83×10^{-8}	1.84×10^{-10}	-3.83×10^{-2}	6.50×10^{-2}	-5.04×10^{-3}	6.5×10^{-5}
0.2	-5.10×10^{-6}	1.33×10^{-7}	-.153	.181	-2.54×10^{-2}	1.45×10^{-3}
0.3	-1.04×10^{-4}	6.23×10^{-6}	-.344	.325	-6.86×10^{-2}	8.77×10^{-3}
0.4	-8.75×10^{-4}	9.42×10^{-5}	-.606	.430	-.136	3.07×10^{-2}
0.5	-4.09×10^{-3}	8.43×10^{-4}	-.942	.617	-.232	7.71×10^{-2}
0.6	-1.44×10^{-2}	5.21×10^{-3}	-1.337	.701	-.310	.151
0.7	-4.37×10^{-2}	2.12×10^{-2}	-1.78	.663	-.362	.227
0.8	-9.73×10^{-2}	6.29×10^{-2}	-2.18	.378	-.319	.194
0.9	-1.43×10^{-1}	1.20×10^{-2}	-2.41	-.556	+.082	-.405
1.0	-	-	-	$-\infty$	∞	$-\infty$

TABLE 3 (Cont'd)

VALUE OF COEFFICIENTS AS A FUNCTION OF THE MEAN RADIUS FOR BUBBLE GROWTH IN THE VICINITY OF A WALL

R_o	$\frac{d\Phi_2^{(3)}}{dR_o}$	$\frac{d\Phi_3^{(4)}}{dR_o}$
0.0	0	0
0.1	-2.13×10^{-6}	1.84×10^{-10}
0.2	-1.91×10^{-4}	1.33×10^{-7}
0.3	-2.60×10^{-3}	6.23×10^{-6}
0.4	-1.63×10^{-2}	9.42×10^{-5}
0.5	-5.28×10^{-2}	8.43×10^{-4}
0.6	-.180	5.21×10^{-3}
0.7	-.414	2.12×10^{-2}
0.8	-.640	6.29×10^{-2}
0.9	-.001	.120
1.0	-	-

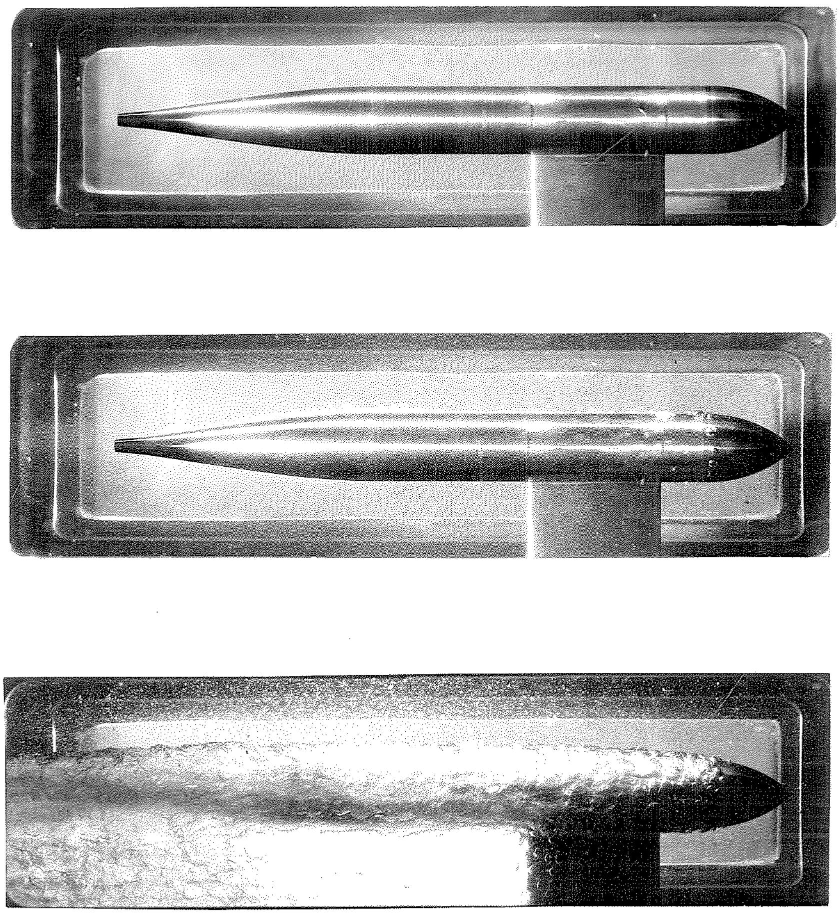

Fig. 1 - Views showing the three regimes of flow.

In the top view, the cavitation parameter K = 0.40; in the center K = 0.28; and in the bottom K = 0.18.

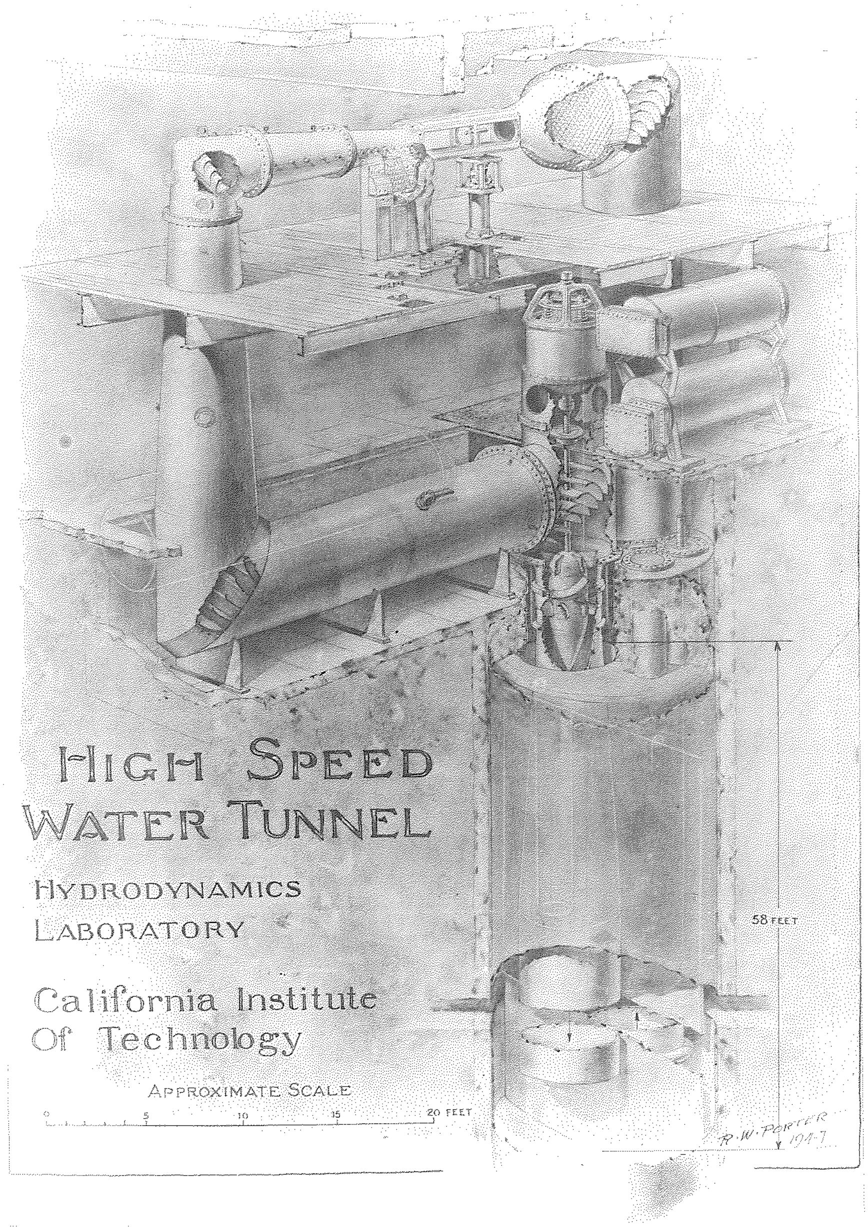

Fig. 2 - Sketch of the High Speed Water Tunnel in the Hydrodynamics Laboratory of the California Institute of Technology.

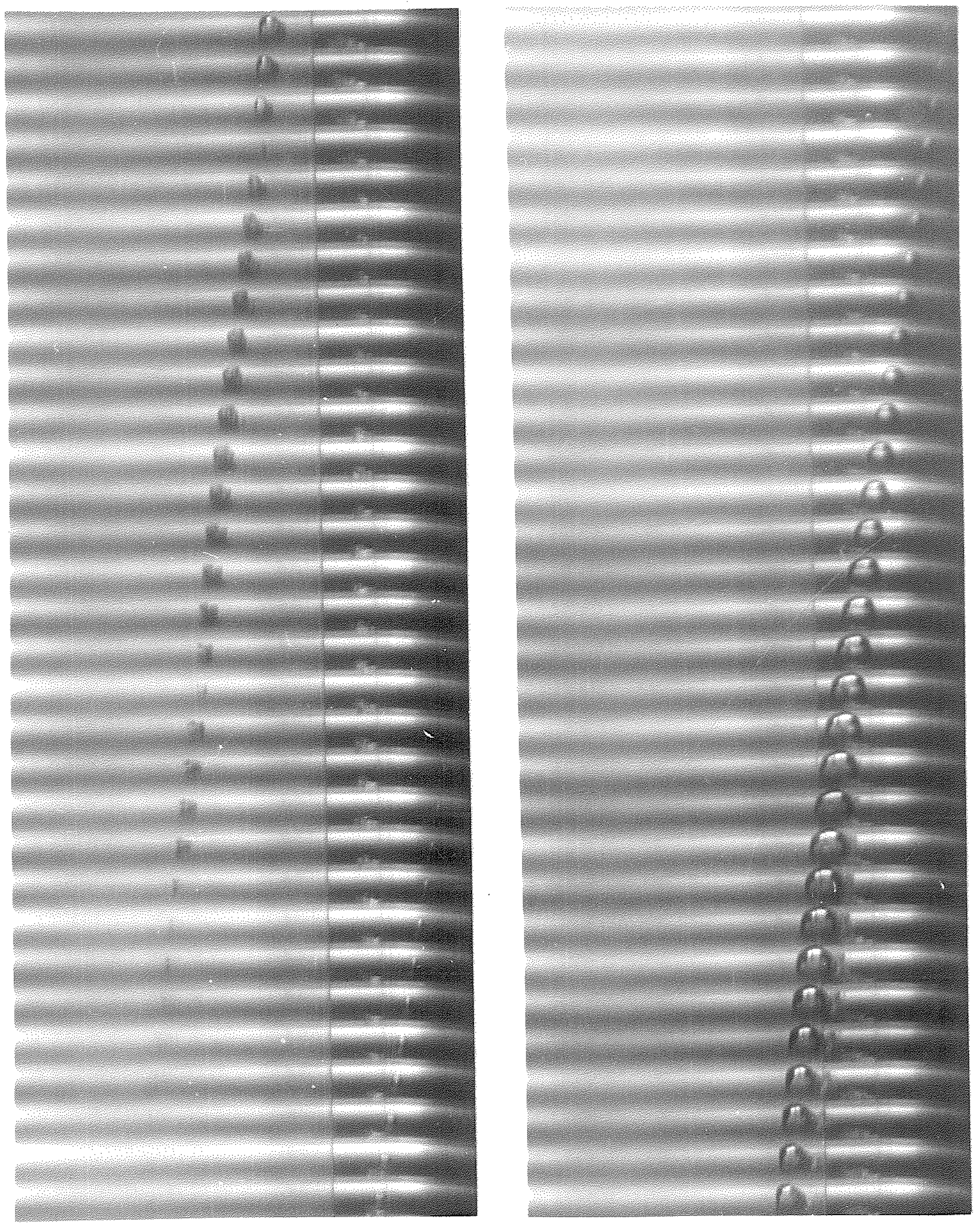

Fig. 3 - Motion of cavitation bubble as observed by Knapp and Hollander [11].

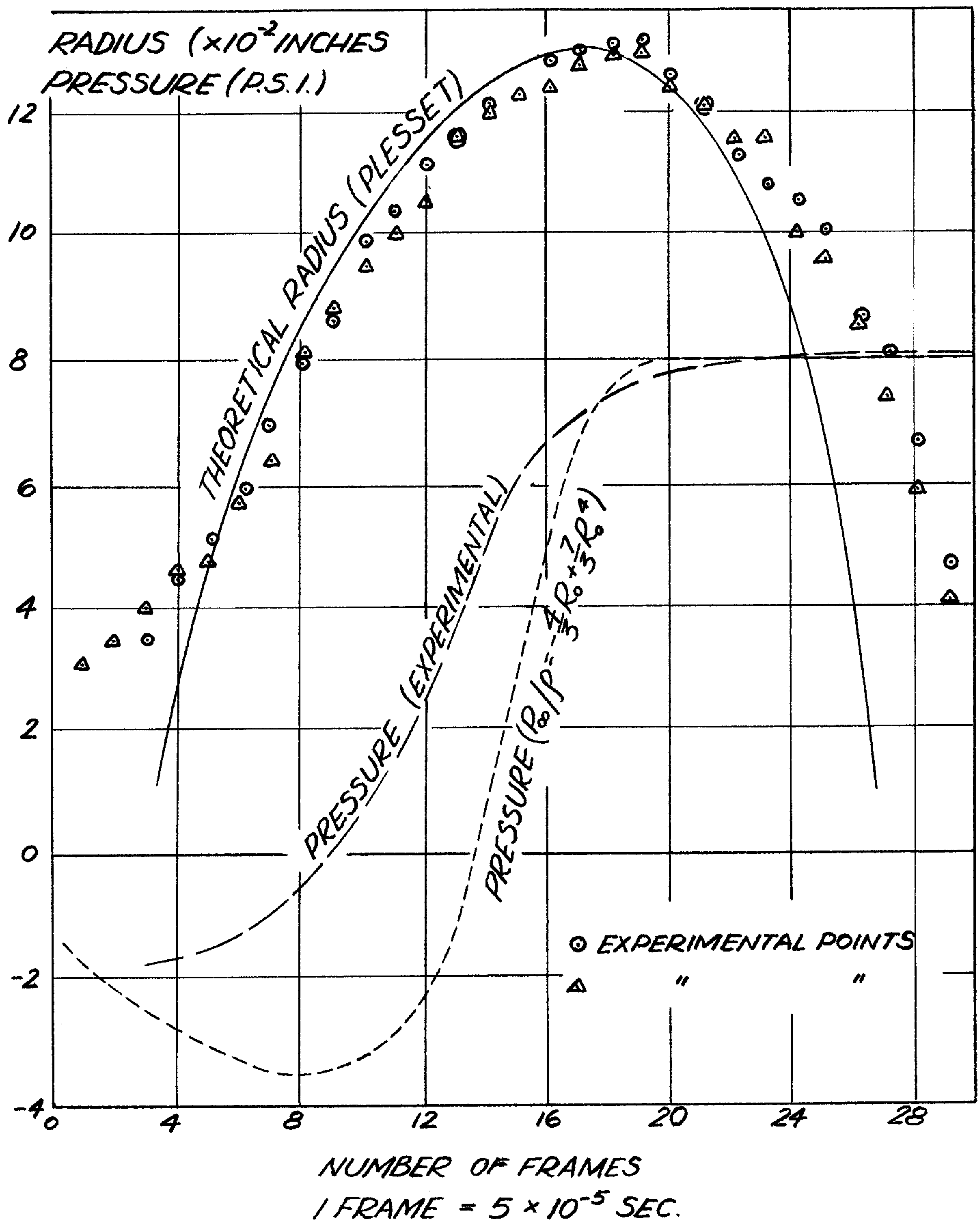

Fig. 4 - Comparison between Plesset's theoretical motion and experimental motion.

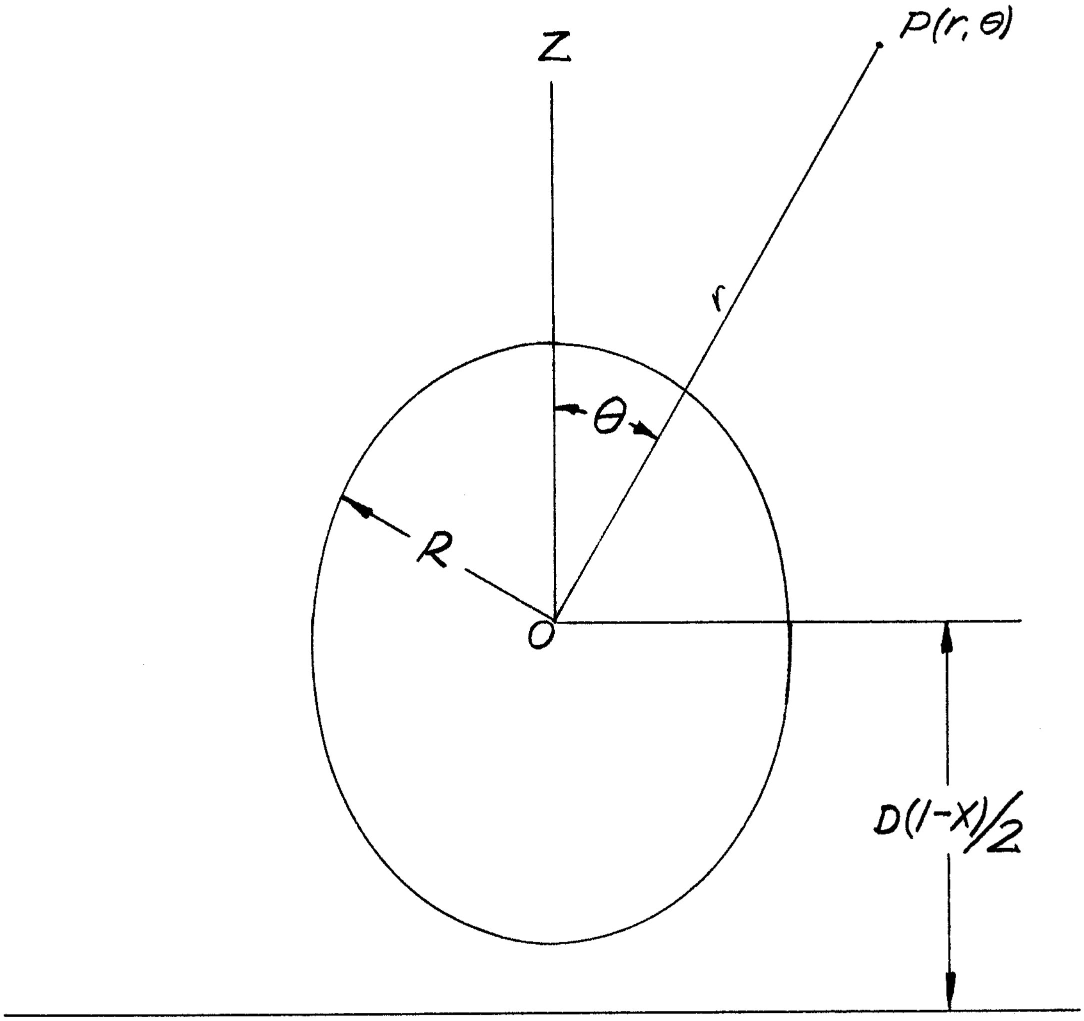

Fig. 5 - Coordinate system for bubble motion in the vicinity of a wall.

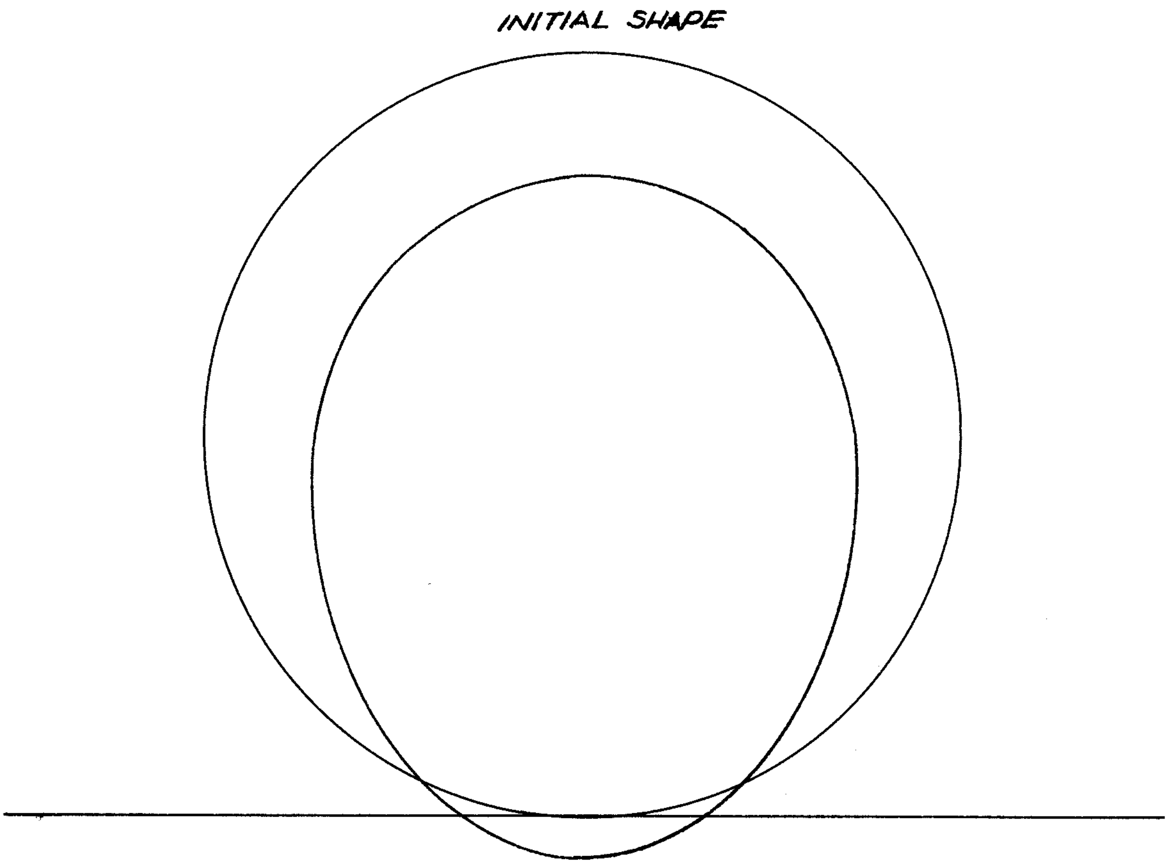

Fig. 6a - Theoretical bubble shape for collapse in the vicinity of a wall, with h = 1/2 and R_o=.75.

Coefficients used are $R_2^{(3)}$, $R_2^{(4)}$, $R_3^{(4)}$, $R_3^{(5)}$, $R_4^{(5)}$, $R_4^{(6)}$, $X^{(3)}$, and $X^{(4)}$.

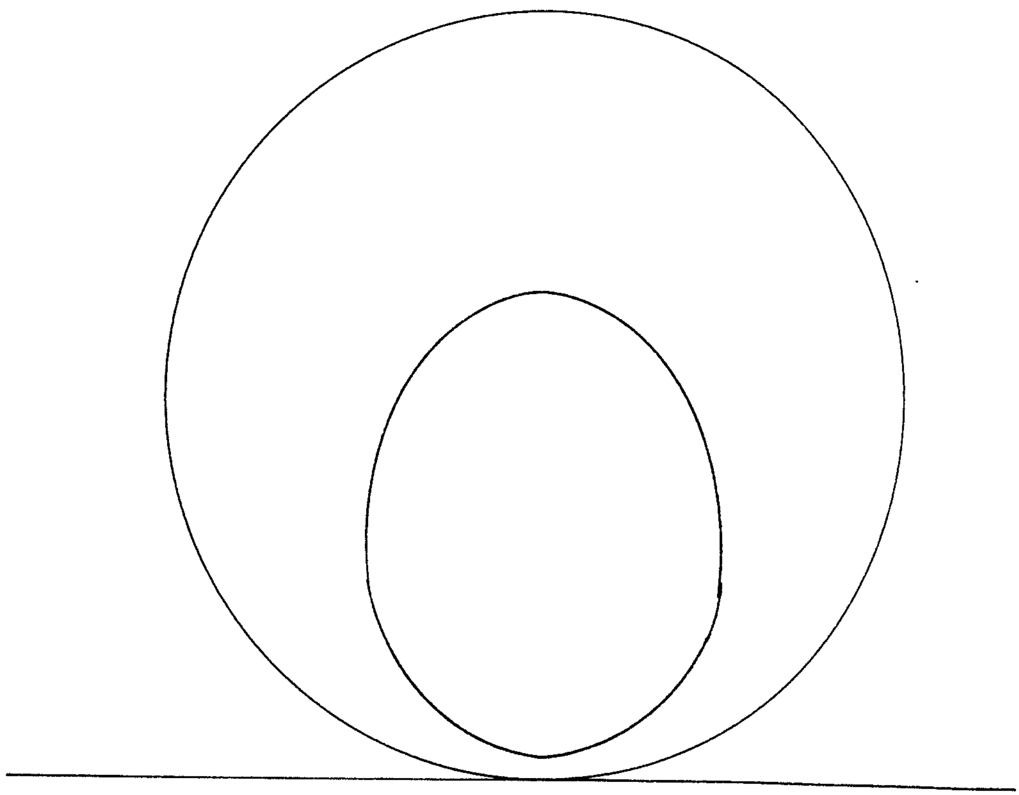

Fig. 6b - Theoretical bubble shape for collapse in the vicinity of a wall, with $h = 1/2$ and $R_o = .5$.

Coefficients used are $R_2^{(3)}$, $R_2^{(4)}$, $R_3^{(4)}$, $R_3^{(5)}$, $R_4^{(5)}$, $R_4^{(6)}$, $X^{(3)}$, and $X^{(4)}$.

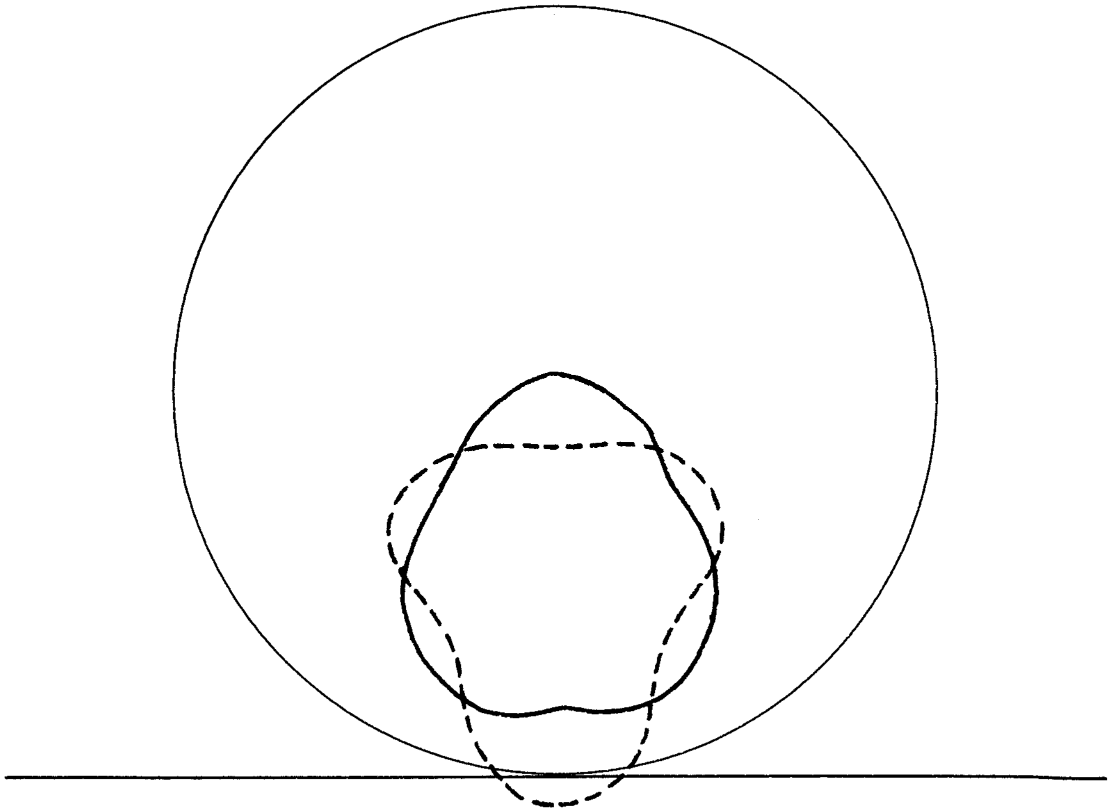

Fig. 6c - Theoretical bubble shape for collapse in the vicinity of a wall with $h = 1/2$ and $R_o = .4$.

Coefficients used are $R_2^{(3)}$, $R_2^{(4)}$, $R_3^{(4)}$, $R_3^{(5)}$, $R_4^{(5)}$, $R_4^{(6)}$, $X^{(3)}$, and $X^{(4)}$. The dotted figure is calculated with the additional use of $R_2^{(5)}$ and $R_3^{(6)}$.

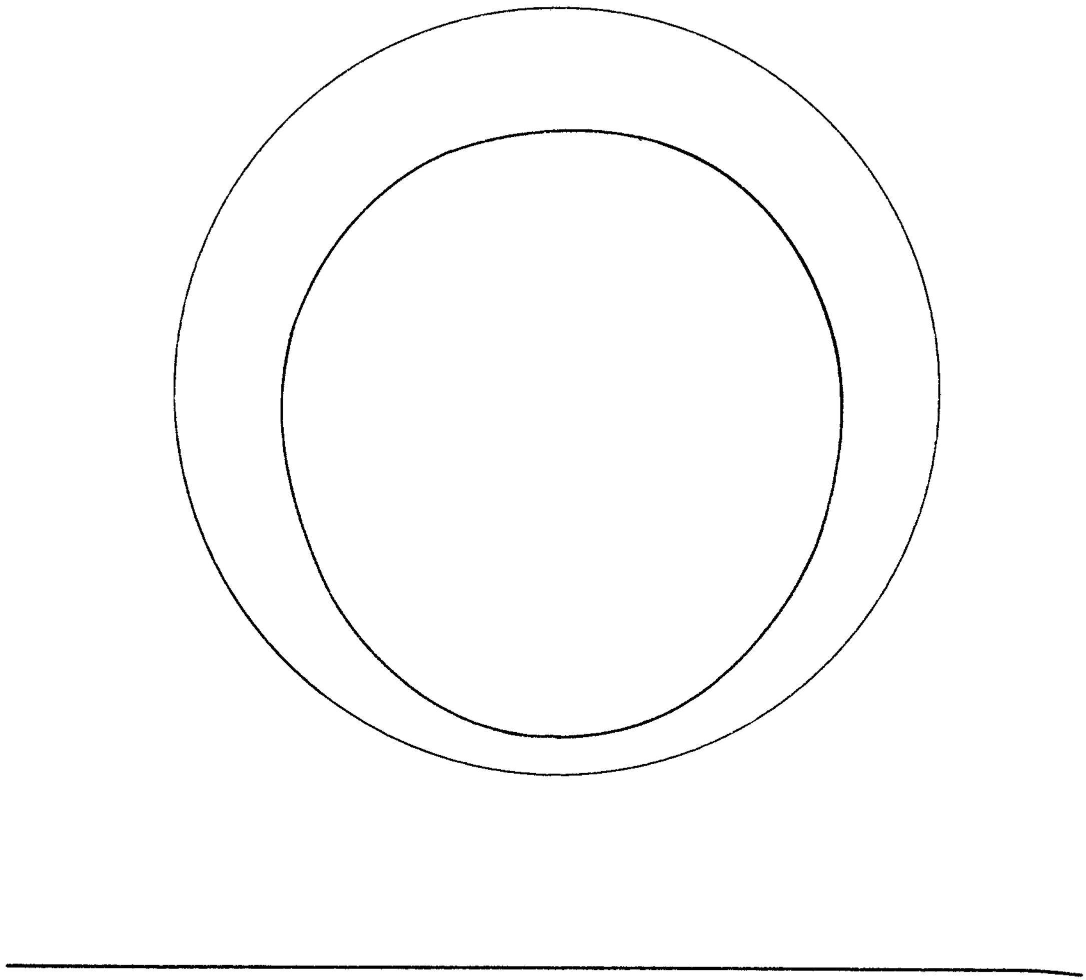

Fig. 7a - Theoretical bubble shape for collapse in the vicinity of a wall, with h = 1/3 and R_o=.75.

Coefficients used are $R_2^{(3)}$, $R_2^{(4)}$, $R_3^{(4)}$, $R_3^{(5)}$, $R_4^{(5)}$, $R_4^{(6)}$, $X^{(3)}$, and $X^{(4)}$.

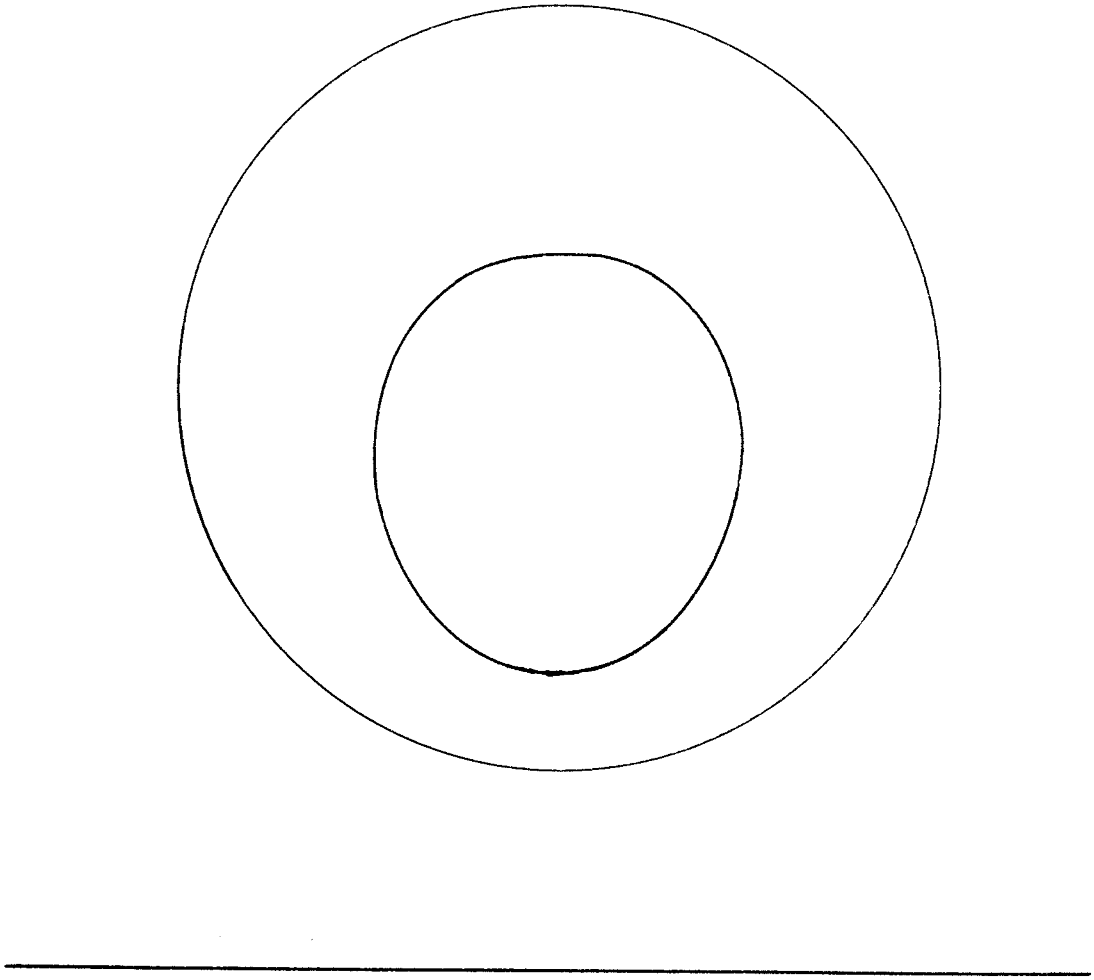

Fig. 7b - Theoretical bubble shape for collapse in the vicinity of a wall, with $h = 1/3$ and $R_o = .5$.

Coefficients used are $R_2^{(3)}$, $R_2^{(4)}$, $R_3^{(4)}$, $R_3^{(5)}$, $R_4^{(5)}$, $R_4^{(6)}$, $X^{(3)}$, and $X^{(4)}$.

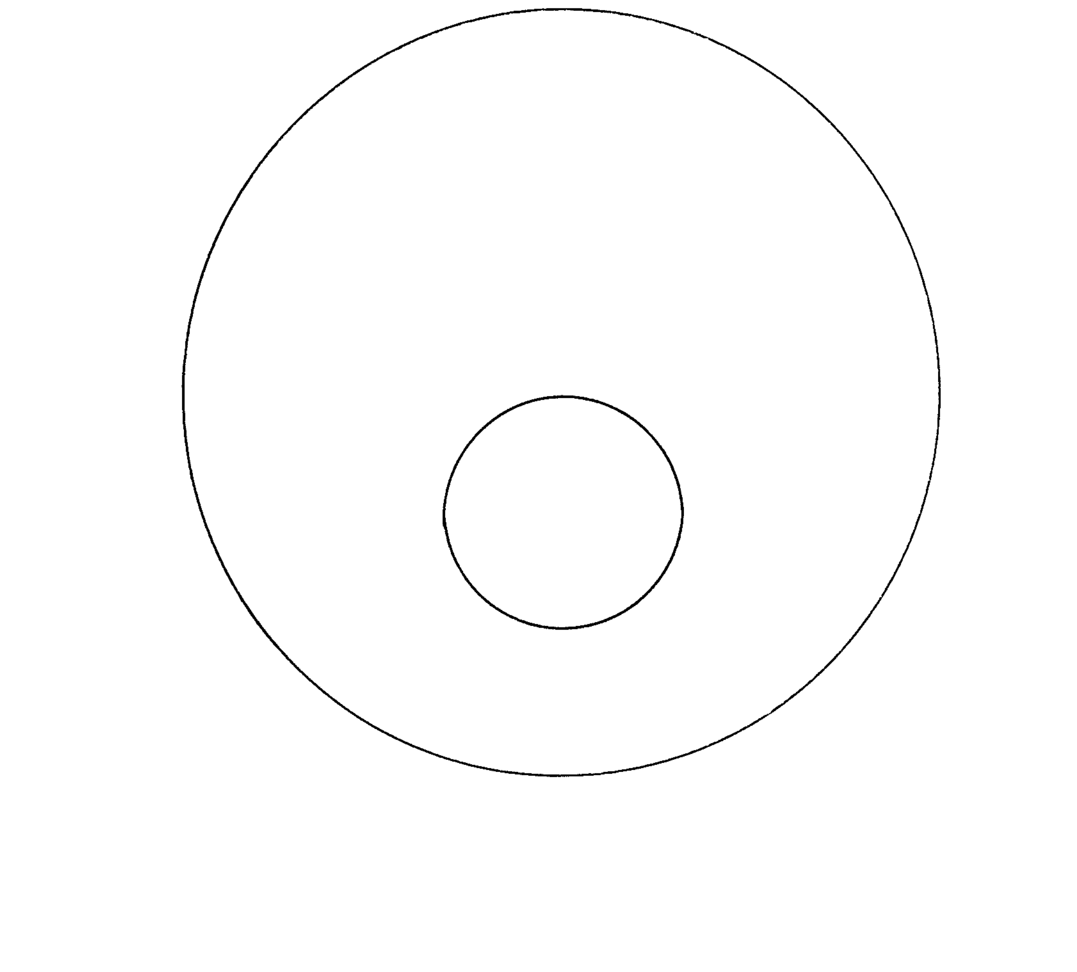

Fig. 7c - Theoretical bubble shape for collapse in the vicinity of a wall, with $h = 1/3$ and $R_o = .3$.

Coefficients used are $R_2^{(3)}$, $R_2^{(4)}$, $R_3^{(4)}$, $R_3^{(5)}$, $R_4^{(5)}$, $R_4^{(6)}$, $X^{(3)}$, and $X^{(4)}$.

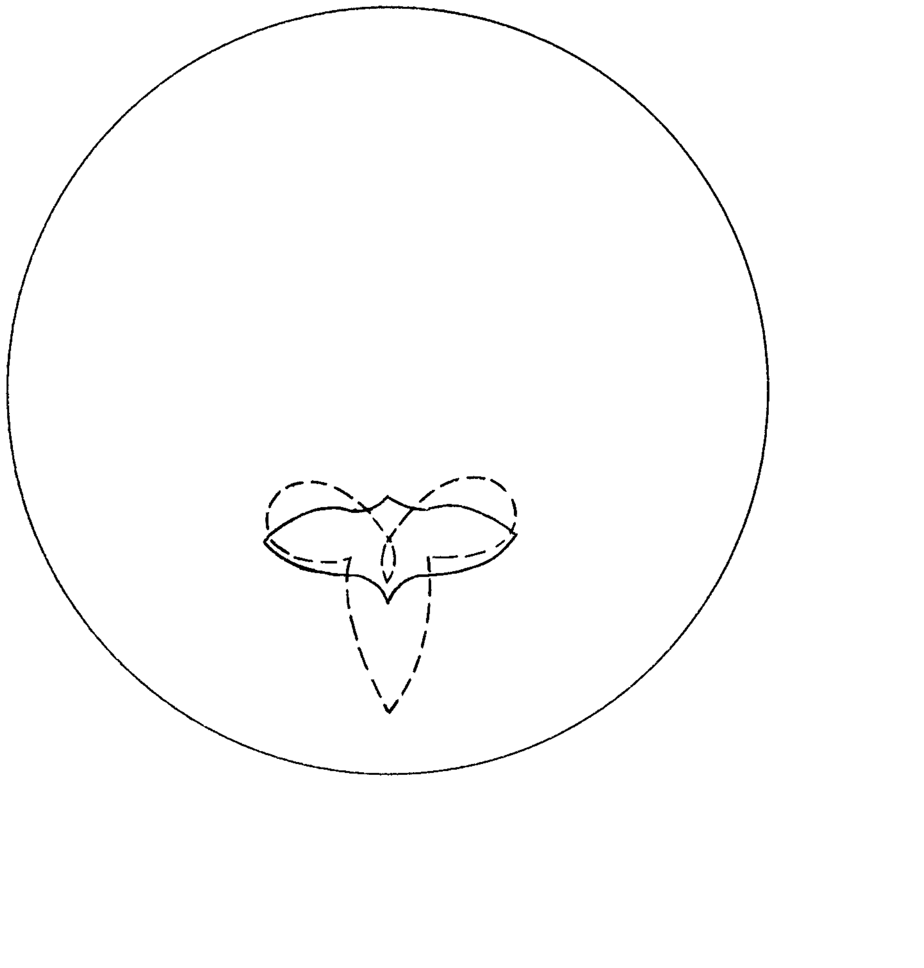

Fig. 7d - Theoretical bubble shape for collapse in the vicinity of a wall, with $h = 1/3$ and $R_o = .2$.

Coefficients used are $R_2^{(3)}$, $R_2^{(4)}$, $R_3^{(4)}$, $R_3^{(5)}$, $R_4^{(5)}$, $R_4^{(6)}$, $X^{(3)}$, and $X^{(4)}$.

The dotted figure is calculated with the additional use of $R_2^{(5)}$ and $R_3^{(6)}$.

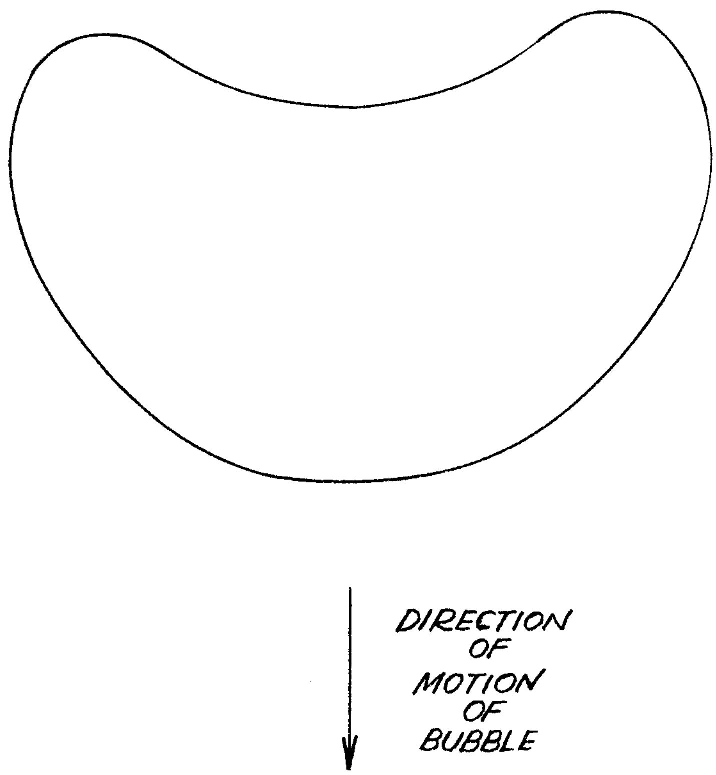

Fig. 8 - Sketch of oscillating gas bubble at its minimum radius with translatory motion of the bubble. (See Ref. 20).

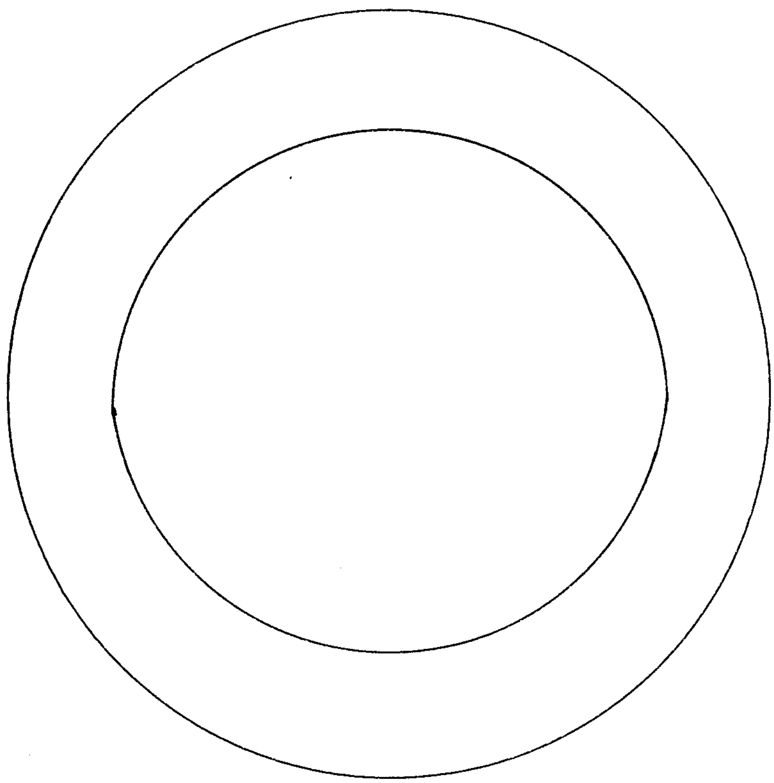

Fig. 9a - Theoretical bubble shape for collapse with translatory motion of the bubble, with $k = 1/10$ and $R_o = .7$.

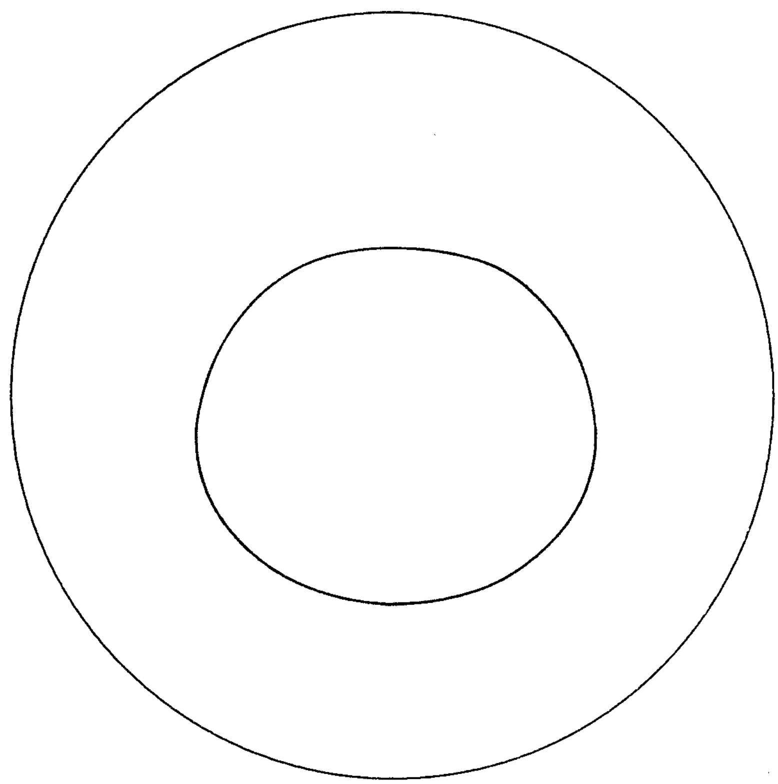

Fig. 9b - Theoretical bubble shape for collapse with translatory motion of the bubble, with $k = 1/10$ and $R_o = .5$.

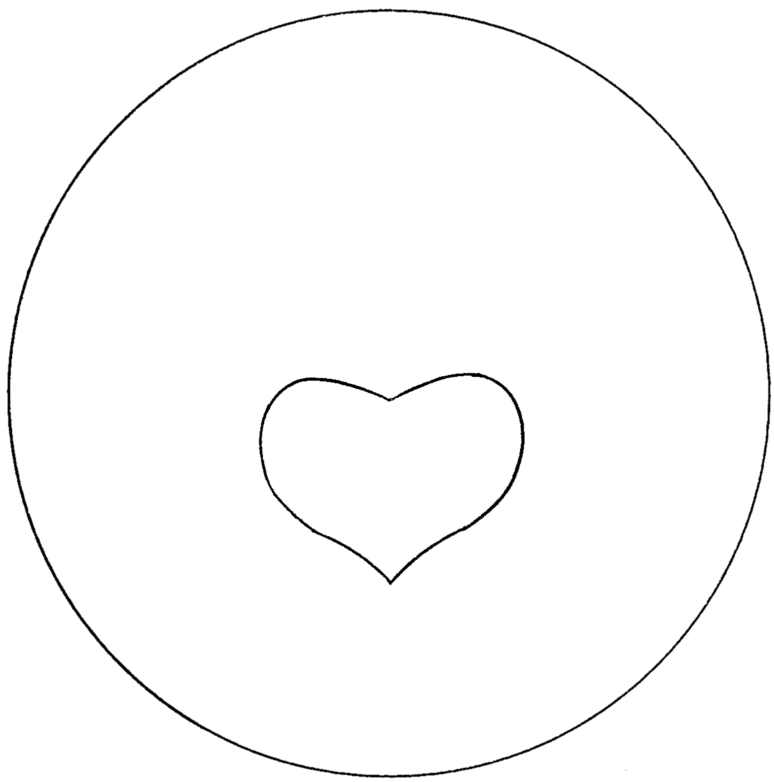

Fig. 9c - Theoretical bubble shape for collapse with translatory motion of the bubble, with $k = 1/10$ and $R_o = .3$.